EUROPEAN RESPIRATORY *journal*

FLAGSHIP SCIENTIFIC JOURNAL OF ERS

Early View

Original article

Targeting HIF2α-ARNT hetero-dimerisation as a novel therapeutic strategy for Pulmonary Arterial Hypertension

David Macias, Stephen Moore, Alexi Crosby, Mark Southwood, Xinlin Du, Huiling Tan, Shanhai Xie, Arlette Vassallo, Alex JT Wood, Eli M Wallace, Andrew S Cowburn

Please cite this article as: Macias D, Moore S, Crosby A, *et al*. Targeting HIF2α-ARNT hetero-dimerisation as a novel therapeutic strategy for Pulmonary Arterial Hypertension. *Eur Respir J* 2020; in press (https://doi.org/10.1183/13993003.02061-2019).

This manuscript has recently been accepted for publication in the *European Respiratory Journal*. It is published here in its accepted form prior to copyediting and typesetting by our production team. After these production processes are complete and the authors have approved the resulting proofs, the article will move to the latest issue of the ERJ online.

Targeting HIF2α-ARNT hetero-dimerisation as a novel therapeutic strategy for Pulmonary Arterial Hypertension

David Macias[1*], Stephen Moore[2*], Alexi Crosby[2], Mark Southwood[3], Xinlin Du[4], Huiling Tan[4], Shanhai Xie[4], Arlette Vassallo[2], Alex JT Wood[2], Eli M Wallace[4], and Andrew S Cowburn[2,5#]

[1]*CRUK Cambridge Centre Early Detection Programme, Department of Oncology, Hutchison/MRC Research Centre, University of Cambridge, Cambridge, United Kingdom;*

[2]*Department of Medicine, University of Cambridge, Cambridge CB2 2QQ, United Kingdom;*

[3]*Department of Pathology, Papworth Hospital National Health Service Foundation Trust, Cambridge CB23 3RE, United Kingdom;*

[4]Peloton Therapeutics Inc., Dallas, Tx, USA, A Subsidiary of Merck & Co., Inc., Kenilworth, NJ, USA.

[5]National Heart and Lung Institute, Imperial College London, ICTEM Building, Hammersmith Campus. Du Cane Road. London. W12 0NN. UK.

[#]To who correspondence may be addressed:

Dr Andrew S Cowburn,

National Heart and Lung Institute,

Imperial College London, ICTEM Building,

Hammersmith Campus. Du Cane Road.

London. W12 0NN.

United Kingdom

Email: acowburn@ic.ac.uk

Telephone: +44 (0)20 759 46581

Summary

PAH is a debilitating disease with no cure. There is an unmet need for new transformative therapies. Targeting HIF2α function through inhibiting ARNT heterodimerization reduces many of the clinical symptoms associated with established PH disease in animals

Abstract

Pulmonary Arterial Hypertension (PAH) is a destructive disease of the pulmonary vasculature often leading to right heart failure and death. Current therapeutic intervention strategies only slow disease progression. The role of aberrant HIF2α stability and function in the initiation and development of pulmonary hypertension (PH) has been an area of intense interest for nearly two decades.

Here we determine the effect of a novel HIF2α inhibitor (PT2567) on PH disease initiation and progression, using two pre-clinical models of PH. Haemodynamic measurements were performed followed by collection of heart, lung and blood for pathological, gene expression and biochemical analysis. Blood outgrowth endothelial cells from IPAH patients were used to determine the impact of HIF2α-inhibition on endothelial function.

Global inhibition of HIF2a reduced pulmonary vascular haemodynamics and pulmonary vascular remodelling in both su5416/hypoxia prevention and intervention models. PT2567 intervention reduced the expression of PH associated target genes in both lung and cardiac tissues and restored plasma nitrite concentration. Treatment of monocrotaline exposed rodents with PT2567 reduced the impact on cardiovascular haemodynamics and promoted a survival advantage. *In vitro,* loss of HIF2α signalling in human pulmonary arterial endothelial cells suppresses target genes associated with inflammation, and PT2567 reduced the hyper-proliferative phenotype and over-active arginase activity in blood outgrowth endothelial cells from IPAH patients. These data suggest that targeting HIF2α hetero-dimerization with an orally bioavailable compound could offer a new therapeutic approach for PAH. Future studies are required to determine the role of HIF in the heterogeneous PAH population.

(Word count 247)

Introduction

Oxygen exchange in the lungs requires a fine matching between ventilation and perfusion. Although the lungs are exposed to the highest partial oxygen tension in the body, there are physiological and pathological conditions that result in local low oxygen availability (hypoxia). This local hypoxia is counteracted by the exclusive, unique oxygen sensing capability of the pulmonary vasculature characterised by a profound vasoconstrictive response to diminishing oxygen tension[1]. Regional lung vasoconstriction stimulates a dynamic shift in perfusion to aid maximal capture of oxygen, however prolonged exposure to hypoxia initiates a potent stimulus that leads to pulmonary vascular remodelling that is a hallmark of idiopathic pulmonary fibrosis[2], chronic obstructive pulmonary disease[3] and pulmonary hypertension[4]. In PAH, changes in endothelial cell and smooth muscle cell proliferation, apoptosis, and metabolism result in vascular remodelling and obstruction. The resulting phenotype progressively reduces pulmonary vascular plasticity, identity and compliance thereby increasing pulmonary vascular resistance (PVR) and back-pressure on the right ventricle (RV) leading to RV hypertrophy and ultimately right-heart failure and death[2]. Currently, there is no cure for PAH, with all existing therapies only slowing disease progression with limited impact on mortality. There is, therefore an unmet clinical need to develop novel transformative therapies.

This programmed response to chronic hypoxia (CH) is in part regulated by hypoxia inducible factors (HIFs) that belong to a group of basic helix-loop-helix-PER-ARNT-SIM (bHLH-PAS) proteins that function as transcription factors responding to oxygen and other stress[5]. The HIFs function as heterodimers composed of a constitutively expressed beta HIF-1b/ARNT subunit and a oxygen regulated alpha subunit that includes HIF1α and HIF2α. Each of the subunits contains two PAS domains (PAS-A and PAS-B) that contribute to the stability of the α- and β-heterodimer complex. HIFα activity is controlled post translationally by the concerted action of oxygen, prolyl-hydroxylases (PHDs), and the ubiquitin proteasome system. In normoxia, PHDs hydroxylate HIFα enabling the ubiquitin proteasome system to

bind and rapidly degrade the protein. Under hypoxia, inactive PHDs allow HIFα proteins to accumulate and dimerize with ARNT to form an active transcription factor complex. HIFα stability and function can also be influenced by aberrantly active cytokines, growth factors, metabolites and reduced prolyl-hydroxylase expression, independent of oxygen resulting in a pseudo-hypoxia phenotype[6-9]. Both of these HIFα regulatory pathways contribute to the initiation and progression of idiopathic PAH (IPAH)[10, 11].

Both HIF1α and HIF2α isoforms have been extensively studied in PH. The first direct evidence came from mice hemizygous for either *HIF1α*[12] or *HIF2α*[13]. Pulmonary disease progression following CH exposure was substantially delayed in these models. Subsequent studies identified tissue-specific HIFα expression in the pulmonary vasculature where HIF2α was found to be highly expressed in the endothelium[14, 15]. We recently reported that genetic ablation of pulmonary endothelial HIF2α prevented the initiation and development of pulmonary vascular remodelling associated with chronic hypoxia-induced PH[16]. Several groups have now reported that endothelial-loss of *PHD2* in mice leads to the aberrant stability of HIF2α with the development of occlusive vascular lesions and severe PH. The concomitant genetic ablation of endothelial *PHD2* and *HIF2α* in this model of PH also inhibited the phenotype, offering near complete protection from PH[8, 9]. These murine gene manipulation studies established HIF2α as the predominant HIFα isoform driving PH. Moreover, patients or mice with HIF2α-gain-of-function mutation have elevated pulmonary haemodynamic associated with PH, further demonstrating that aberrant stability of HIF2α can initiate this disease[17, 18]. Although substantial progress has been made unravelling the role of HIF2α in PH, it has taken almost two decades to identify and develop suitable small molecule inhibitors as potential candidates for PH therapy.

As a transcription factor that activates gene expression through protein-protein interactions, HIF2α was generally regarded as intractable for small molecule inhibition. However, biophysical studies by Bruick, Gardner and colleagues[19] led to the discovery that the inner core of the PAS-B domain of HIF2α possess a hydrophobic cavity that can bind small

molecules that allosterically disrupt its dimerization to ARNT and thereby block transcriptional activity. Independently, Zimmer et al[20] used a cellular screening approach to identify HIF2α inhibitors that resulted in the discovery of Compound 76 (C76). C76 inhibits HIF2α translation by binding to the iron regulatory protein. While the latter approach led to a molecule that has been used in a handful of preclinical models, it demonstrates only micromolar potency *in vitro*, and has not been shown to be orally bioavailable. In contrast, the former approach, led to a series of highly selective, orally bioavailable HIF2α inhibitors. These direct HIF2α inhibitors are efficacious in rodent cancer models, and, importantly, demonstrate anti-tumour activity in metastatic clear cell renal cell carcinoma (ccRCC) patients along with a favourable safety and tolerability profile[21-25]. As such, given that HIF2α is a potent stimulus of pulmonary vascular remodelling in PH, we evaluated a direct HIF2α inhibitor, PT2567[25] in preclinical PH models. We performed haemodynamic profiling and biochemical analysis of the rodent su5416/hypoxia model using both prevention and intervention strategies with vehicle, PT2567 or sildenafil as a clinically relevant comparative compound. Herein we demonstrate that HIF2α inhibition reduces haemodynamic parameters associated with severe PH development by reversing pulmonary vascular remodelling, decreasing circulating pro-inflammatory factors and by restoring plasma nitrite levels, suggesting that inhibition of this critical pathway could provide a promising new strategy in the treatment of PH.

Methods

Animals: This research has been regulated under the Animals Scientific Procedures Act 1986 amendment regulations 2012 following ethical review by the University of Cambridge Animal Welfare and Ethical Review Body (AWERB) Home Office Project License 70/8850. All animals were housed on a 12 hr. / 12 hr. light-dark cycle with ad-lib standard chow and water. A power calculation determined the number of rats required per group to detect a 25% effect change at 80% power 5% significance level. The group size for the

su5416/hypoxia prevention studies was calculated to be n=10, and the su5416/hypoxia and monocrotaline intervention studies were calculated to be n=15 and n=14 respectively

Sugen5416/hypoxia rat model of PH: Male Sprague Dawley rats (~150 to 200 grams, Charles River) were given a single sub-cutaneous injection of su5416 (20 mg/kg, Tocris, Bristol, UK) in vehicle (0.5% carboxyl methylcellulose sodium, 0.4% polysorbate 80, 1% Benzyl alcohol 5% DMSO 5% PEG 400, all Sigma), placed immediately into a 10% O_2 chamber and maintained in hypoxia for 3 weeks. Depending on the treatment strategy, Rats assigned to the prevention protocol were randomly assigned to 4 treatment groups and received vehicle, PT2567 (100mg/kg or 300mg/kg) by oral gavage *q.d. (once-a-day)* or sildenafil (30mg/kg) *b.i.d* (twice-a-day) during the hypoxic exposure. Rats assigned to the intervention protocol were allowed to acclimate to normoxia for 24hr before being randomly assigned to 3 groups for treatment with vehicle, PT2567 (100mg/kg) by oral gavage *b.i.d (twice-a-day)* and Sildenafil (30mg/kg) by oral gavage *b.i.d (twice-a-day)* for 3 weeks. Cardiac echo, Right ventricle systolic pressure and right ventricle hypertrophy were measured as previously described[26-28]. Cardiac echo parameters were measured using a (Vevo® 3100 imaging System, FUJIFILM VisualSonics Inc. Toronto, Canada). A parasternal long axis view of the left ventricle was obtained in order to visualise the left ventricle, aorta and mitral valve leaflets. The pulmonary artery was visualised and colour Doppler confirmed correct placement of a pulse wave Doppler within the maximum flow velocity. Peak velocity of the pulmonary artery was measured to determine pulmonary outflow along with the right ventricle outflow tract velocity time interval (RVOT-VTI). Pulmonary acceleration time (PA-AT, defined as the time from the onset of flow to peak velocity by pulsed-wave Doppler recording), and right ventricular ejection time (PA-ET, the time from the onset to the termination of pulmonary flow) was measured. An Apical four-chamber view was obtained to quantify the blood flow spectrum and characterise peak tricuspid regurgitation velocity (if present) (TRV). An estimate of pulmonary vascular resistance (PVR) was calculated using the formula PVR(WU) = 10 X TRV/RVOT-VTI. All echocardiograms were performed by the

same individual and analysis was performed offline and the individual was blinded to the treatment group. After, heart, lung and blood were taken for histological, gene expression and biochemical analysis.

Monocrotaline rat model of PH: Male (Sprague Dawley) rats (100 to 125 grams, Charles River) were randomly allocated to 4 groups and injected subcutaneously with either vehicle control (0.9% saline) at 2mL/kg or 40mg/kg (2mL/kg) Monocrotaline (MCT) (sigma-Aldrich - PHL89251) as previously described[26]. Fourteen days post MCT or vehicle injection animals underwent a baseline cardiac echo (Vevo® 3100 imaging System, FUJIFILM VisualSonics Inc. Toronto, Canada) in order to ascertain disease severity. Echocardiograms were performed by the same individual and blinded to the treatment groups. All analysis was performed offline. The animal treatment groups were as follows: group 1 vehicle-non disease control (CMC in 0.9%Saline); group 2 vehicle disease control (CMC in 0.9%Saline); group 3 HIF2α-inhibitor intervention (PT2567 100mg/kg) oral gavage *b.i.d (twice-a-day)* group 4 sildenafil intervention (30mg/kg) by oral gavage *b.i.d (twice-a-day)* for 2 weeks

Following the dosing period all animals underwent cardiac echo as previously described above.

Pulmonary Vascular Morphometry: Lung were inflated and fixed via the trachea with 4% PFA at a constant fluid pressure of 15-20cm for 5 mins. Lungs from the prevention protocol were stained for elastin/eosin, and the intervention protocol stained with hematoxylin and eosin, elastic van Gieson (EVG) stain to assess histology (MSD/BDH, Lutterworth UK). Histological findings were assessed by a blinded independent pathologist who scored the lung sections for perivascular/vascular inflammation, perivascular fibrosis and smooth muscle hypertrophy of small arterioles. The findings were recorded as 0 (normal), 1 (minimal), 2 (mild), 3 (moderate), 4 (marked). Scoring of smooth muscle hypertrophy in pulmonary arterioles was based on thickness of the muscle wall and the extent of the finding (apparent number of arterioles affected). Serial lung sections from the intervention protocol

were also immunostained with anti-smooth muscle α-actin (α-SM actin; DakoCytomation Ely UK), von Willebrand factor and anti-MPO (DakoCytomation), and anti-Ki67 (abcam) to assess the degree of muscularization of small pulmonary arteries (≤50μm), cellular proliferation and myeloperoxidase positive cells. Antibody staining was visualised using 3-3' diaminobenzidine hydrochloride substrate (DakoCytomation) and counterstained with Carrazzi hematoxylin (Bios Shelmersdale UK). Vessel medial thickness was measured using Image J software (MediaCybernetics, Bethesda MD). Tissue samples were independently coded and quantified by a blinded pathologist.

Haematological Analysis: Anti-coagulated blood was analysed using Vet abc haematology analyser (Horiba) according to the manufacturer's instructions. Cytokine and growth factor profiling was undertaken in plasma isolated from anticoagulated whole blood which had undergone centrifugation at 1500g for 5 mins and frozen to -80ºC.

Nitrite Analysis: Blood samples were centrifuged to separate plasma and were passed through a column with a 10-kDa cut-off filter. All samples were analysed for nitrite content using a NOA 280i (Siever, GE Healthcare) according to the manufacturers instructions

RNA Analysis**:** Total RNA was isolated from tissues using TRI-reagent (Sigma) followed by RNA clean-up and DNase digest using RNeasy column kits (Qiagen). First-strand synthesis was performed with 1μg of total RNA using Superscript IV (Invitrogen) according to the manufacturers instructions. Relative gene expression was determined by quantitative PCR (qPCR) (One-Step Plus Real-Time PCR System; Life Technologies) and was amplified in SYBR-Green master mix (Roche) and relevant primers from Qiagen. Relative gene-expression levels were corrected to house keeping genes β-actin and B_2M.

Carotid Body Histology: The carotid bifurcation was dissected, fixed for 2 hr. with 4% paraformaldehyde (Santa Cruz Biotechnology) and cryopreserved (30% sucrose in PBS) for cryosectioning (10 μm thick, Bright Instruments, Luton, UK). Tyrosine hydroxylase (TH), was detected using rabbit anti-TH (1:5000, Novus Biologicals, Abindong, UK; NB300-109)

primary antibody and Alexa-Fluor 568-conjugated anti-rabbit IgG (1:500, ThermoFisher, Waltham, MA US).

CB area was measured on micrographs (Leica DM-RB, Wetzlar, Gernany) taken from sections spaced 60 µm apart across the entire CB using Fiji

software[29]. CB volume was estimated according to Cavalieri's principle as previously reported[30] Tissue samples were coded and quantified by a blinded investigator.

PT2567 SD Rat Pharmacokinetics: PT2567 was suspended in methylcellulose Tween-80 (0.5% methylcellulose, 0.5% Tween-80 in water) and rats (n=3 per dose level) were dosed by oral gavage. Blood samples were taken at 0.25, 0.5, 1, 2, 4, 8, 12 and 24 h post dose. Plasma PT2567 concentrations were conducted by non-compartmental method using Pharsight WinNonlin. A non-compartmental model was used to analyse the data.

BOECs Isolation Culture: BOECs were isolated from the blood of participants previously diagnosed with PAH or from normal, healthy volunteers at the Addenbrooke's University of Cambridge teaching hospital National Health Service Foundation Trust, Cambridge, United Kingdom, following a protocol approved by the Cambridge Research Ethics Committee (REF:11/EE/0297). Table 1 contains characteristics of PAH patients and information of the healthy volunteers. Mononuclear cells were isolated from 60 mL of venous blood by Ficoll density gradient centrifugation and plated onto type 1 rat tail collagen-coated (BD Biosciences) flasks in endothelial selective medium (EGM2; Lonza Biologics) supplemented with 10% ES-screened FCS and additional growth factors (EGM2 bullet kit; Lonza Biologics). BOECs appeared after 2–3 wk and were subsequently passaged when confluent.

Table-1 PAH patient characteristic for the isolation of BOECs

BOEC's were cultured for a maximum of 5-passages. For BOEC hypoxic exposure experiments, cells were transferred to a Baker-Ruskin hypoxic chamber (Bridgend UK), pre-hypoxic media was transferred into each well +/- inhibitors. Cell were cultured under 1% O_2 for the experimental times indicated in the results

	Age	Sex	Ethnicity	mPAP (mm/Hg)	CI (L/min/m^2)	PVR (WU)	6min walk (m)	Treatment	PAH class
PAH	45	M	Caucasian	46	1.75	9.7	381	ERA, PDEI	Heritable
PAH	79	F	Caucasian	52	2.25	10.96	124	PDEI	Idiopathic
PAH	32	M	Caucasian	60	2.69	10.8	400	PGI, PDEI	Heritable
Control	30	M	Caucasian						
Control	37	F	Caucasian						
Control	41	M	Caucasian						

Cell Culture: 786-O and Hep3B cell lines were purchased from ATCC. Cells were cultured in DMEM with 10% FBS. Human PAEC were purchased from Promocell and cultured in endothelial cell growth medium. For PT2567 treatment cells were plated into 6-well plates. PT2567 dissolved in DMSO was added as the cultures reach confluence with a final concentration of DMSO at >0.1%. For hypoxia-treated cells, cell culture media was exposed to 1% O_2 5% CO_2 (Ruskin) for 12 h before transferring onto cells. Following the addition of PT2567 the cells were maintained under hypoxia for the duration of the treatment.

Arginase Activity Assay**:** BOECs were prepared as described above. Urea production was normalized with protein concentration.[31]

Knockdown experiments: Control human-PAEC and human BOECs derived from both control volunteers were transduced using lentiviral particles containing three different shRNAs targeting human HIF-1α, and HIF-2α, mRNA respectively. shRNA sequences were selected from The RNAi Consortium (TRC) according with the following criteria: those shRNAs seeming to have less potential off-targets binding sites and that were validated by MISSION shRNA Library (Sigma-Aldrich). The individual clones ID selected were TRCN0000003808 (HIF1α), TRCN0000003806 (HIF2α), TRCN0000342501. Oligos for each individual shRNA were annealed and cloned into pLKO.1 plasmid following TRC recommendations. Positive colonies were checked by sequencing. To produce lentiviral vectors, Lenti-X 293T cells (Clontech) were cotransfected with single pLKO.1, pCMV-

dR8.91 and pMD2.G plasmids using Lipofectamine 2000 (Thermo-Fisher Scientific) according to the manufacturer's protocol. Lentiviral particles were collected 48 h after transfection and used to transduce human-PAEC and BOECs overnight. Next, fresh media was added and the cells were incubated in normoxia for 2 d then in 1% O_2 atmosphere.

Proliferation assay: BOECs were plated in 24-well plates at 20000 cells per well. Cells received complete EGM-2MV medium with / without PT2567. Cells were counted on days, 0, 2, 4, 6 with trypan blue exclusion.

BOEC endothelial network formation assay: BOEC from PAH patients and healthy volunteers where grown to 90% confluence. BOECs where transferred into control media or media containing 1μM PT2567 before seeding at approx. 75 000 cells in Matrigel matrix coated 12 well plates. Images were captured 20 hr. after treatment using phase-contrast microscopy (Lieca MZ16). Tube network length and network loop were determined by Image J software (MediaCybernetics, Bethesda MD).

Co-Immunoprecipitation of HIF2α and ARNT: Cells in 6-well plate were lysed in 1 mL of cell lysis buffer (Tris-HCl 20 mmol/L, pH 7.5, Triton X-100 1%, NaCl 150 mmol/L, glycerol 5%, EDTA 1 mmol/L, DTT 1 mmol/L, and 1 tablet per 10 mL of Roche Protease Inhibitor Tablet Complete). A total of 1 μg of mouse mAb against human ARNT (Santa Cruz Biotechnology, sc-55526) or 1 μg of antibody against HIF2α (Abcam Ab199) and 50 μL of Protein AG Beads (Santa Cruz Biotechnology 50% slurry in lysis buffer) were added to cleared cell lysate. The tubes were rotated at 4°C for 16 hours. After washing in cold lysis buffer, the bead-bound proteins were separated by SDS gel electrophoresis and subjected to Western blotting with specific antibodies.

Isothermal titration calorimetry: Human HIF2α-B was expressed and purified as previously described[19]. Rat HIF2α differs from human HIF2α-B by only three amino acids. So, the expression vector for human HIF2α-B was mutated at these residues (T262L, I 265V, and I326V) to make rat HIF2α-B. The binding affinity between PT2567 and PAS-B

domains was determined using ITC on an iTC200 system (GE Healthcare). PAS-B at 0.5 mmol/L was titrated into 26 µmol/L or 25 µmol/L of PT2567 for human or rat respectively in the cell in buffer consisting of 20 mmol/L Tris-HCl, pH 8.0, 150 mmol/L KCl, and 1% DMSO.

Statistical Analysis*:* All data represents the mean (±SD) of *n* separate experiments unless otherwise stated. The difference between groups was assessed using one-way ANOVA with multiple comparison test Tukey. All data was tested for normal distribution. If not normally distributed the non-parametric Kruskal-Wallis test was used with Dunns multiple comparison test, unless otherwise stated. Statistical analysis for the monocrotaline mortality data was assessed by the log-rank (Mantel-Cox) test. Analysis was undertaken using GraphPad Prism Version 7.0 c for Mac OS. A *P* value of <0.05 was considered significant.

Results

HIF2α/ARNT dimerization disruption

We began by determining the binding affinity of PT2567 for human and rat HIF2α PAS-B domain by isothermal titration calorimetry. The K_d for this HIF2α PAS-B domain interaction is 30nM and 29nM for human and rat respectively (Supplemental Figure 1a and b). We next assessed the disruption of HIF2α/ARNT interaction/dimer by co-immunoprecipitation assay in 786-O cells. This ccRCC cell line was selected as it constitutively expresses active HIF2α in normoxia without HIF1α due to truncation of the *HIF1α* gene. Initially we immunoprecipitated ARNT in lysates of 786-O cells treated with PT2567. Immunoblotting shows that ARNT protein co-precipitation with HIF2α is diminished in response to PT2567 treatment in a concentration dependent manner demonstrating disruption of HIF2α/ARNT dimer formation (Supplemental Figure 1c).

Inhibition of HIF2α transcription

We next evaluated the effect of PT2567 on HIF2α-dependent transcriptional activation of target genes by qPCR analysis. Treatment of 786-O cells with PT2567 significantly reduces the mRNA expression for *GLUT1, EPO, CCND1, PAI1, and VEGFA,* in a concentration

dependent manner (Supplemental-Figure 2a-e). We further evaluated the specificity of PT2567 in Hep3B hepatoma cells. Hypoxia leads to the accumulation of both HIF1α and HIF2α protein in this cell line. Treatment of Hep3B cells with PT2567 reduced the hypoxic-induced expression of HIF2α target genes only; *EPO* and *PAI1,* with no effect on HIF1α target gene expression; *PDK1* or *PGK1* (Supplemental-Figure 2f-i). This important data confirmed the target specificity of PT2567, only disrupting HIF2α/ARNT interaction without affecting HIF1α/ARNT transcriptional activity.

PT2567 validation in hPAEC

We next assessed the activity and specificity of PT2567 in primary hPAEC. We initially confirmed HIF1α and HIF2α target genes in these cells through short-hairpin knock-down (shRNA-HIF1α or HIF2α) of these transcription factors followed by timed exposure to hypoxia (Supplemental-Figure 3a-f). We confirmed the near complete inhibition of PAI-1 and partial inhibition of VEGF and GLUT1 mRNA expression in HIF2α$^{-/-}$ PAEC with no effect on HIF1α target LDHA mRNA expression. Treatment of hPAEC with PT2567 markedly reduced the hypoxia-induced expression of HIF2α target genes and PH associated genes; *GLUT1, VEGF, CXCL12, CXCR4, ICAM1, Sele, PAI1, APLN and restored ID1* gene expression in a concentration dependent manner without effecting HIF1α target gene transcripts for *LDHA* and *PDK1* (Supplemental-Figure 3g-q). These results confirm that PT2567 disrupts HIF2α/ARNT interaction without affecting HIF1α/ARNT transcriptional activity in hPAECs.

PT2567 prevents the initiation and development of PH

We next determined the rat plasma pharmokinetic profiles for PT2567. Timed plasma analysis identified both 100mg/Kg and 300mg/Kg oral gavage achieved good exposure (Supplemental-Figure 4a). We initially investigated the effect of PT2567 on PH development with a prevention protocol using the rat su5416/Hx model. Rats were randomly assigned to 4 treatment groups, received a single *s.c.* dose of su5416 and then housed in 10% O_2 for four weeks. The rats received vehicle, PT2567 (100mg/kg or 300mg/kg) *q.d. (once-a-day)*

or sildenafil (30mg/kg) *b.i.d* (twice-a-day) by oral gavage (Supplemental-Figure 4b). The development and progression of pulmonary hypertension was assessed through measurement of right ventricular systolic pressure (RVSP). RVSP in both PT2567 treatment groups was significantly lower, in a dose-dependent manner (43.22± 20.72mmHg and 30.78± 11.07mmHg, respectively for 100 and 300 mg/kg groups) compared to vehicle (72.83± 18.14mmHg). In contrast, sildenafil treatment only showed a modest blunting of RVSP, not significantly different from vehicle (56.10± 17.55mmHg) (Figure 1a). The Fulton index (RV/LV+S), as an indicator of right ventricle hypertrophy (RVH), was also lower in PT2567 treated animals (0.421±0.100 and 0.350±0.06, respectively for 100 and 300 mg/kg groups) when compared to vehicle (0.578±0.13)(Figure 1b). Sildenafil treatment provided only little protection from RVH (0.5220±0.14)(Figure 1b). Consistent with the data described above, there is a positive correlation between RVSP and RVH (r^2=0.666, p<0.0001) (Supplemental-Figure 4c). Final body weight across all treatment groups did not deviate from vehicle controls (Supplemental-Figure 4d).

Assessment of pulmonary histopathology is presented in supplemental table 1a. Smooth muscle hypertrophy associated with distal pulmonary vessels (≤50μm), perivascular/vascular inflammation and perivascular fibrosis scoring was greatest in vehicle treated group (5.42), meanwhile there was a dose dependent decreased score in animals treated with PT2567 100mg/kg (3.66) and 300mg/kg (2.55) respectively. Sildenafil group scored higher (4) than PT2567 treated animals. Additionally, we quantified vessels muscularisation and observed a decreased percentage of fully muscularised arterioles accompanied by an increase in non-muscularised arterioles in animals treated with PT2567 compared with vehicle or sildenafil treated groups (Figure 1c-d and Supplemental-Figure 4 e-g).

We next assessed the extent of small arterial occlusion. Vessels (≥50μm) were determined to be either fully occluded or with an open lumen. We observed a decrease in the percentage of occluded vessels in both PT2567 (100mg/kg and 300mg/kg) treated groups compared to vehicle and sildenafil treated groups (Figure 1e).

Intervention with PT2567 decreases PVR in established PH

We next evaluated whether an intervention strategy with PT2567 (100mg/kg) would influence pulmonary vascular function and PH disease progression in su5416/hypoxia rats. As illustrated in Supplemental-Figure 5a all rats received the same su5416/hypoxia initiation process as described in the prevention protocol. Haemodynamic baseline was assessed 24hr after removal from the hypoxic chamber. These data provide a point of reference of disease severity for the intervention arms of the study. The remaining rats were randomly assigned to 3 groups for treatment with vehicle, PT2567 (100 mg/kg) or sildenafil (30 mg/kg) by oral gavage *b.i.d (twice-a-day)* for 3 weeks. Normoxic-control groups received vehicle or PT2567 treatment for 3-weeks. Haemodynamic analysis of the intervention arm was then completed 16-18hr after the final oral gavage. We believe this time delay facilitates the assessment of pulmonary vascular stasis rather than the vaso-tensive modulating properties of the compounds. We report RVSP in the PT2567 group (64.85±16.86mmHg $p<0.05$) was significantly lower than vehicle control (89.82±27.92mmHg)(Figure 2a). Sildenafil (77.29±26.56mmHg) did not lower RVSP when compared to vehicle treated rats. The Fulton index (RVH) was also significantly lower in PT2567 treated group (0.4074±0.079) compared to vehicle alone (04906±0.098)(Figure 2b), a strong correlation was noted between RVSP and RVH ($r^2=0.7066$, $p<0.0001$) (Supplemental-Figure 5b). Notably, PT2567 treatment significantly influenced the restoration of cardiac output (CO)(Figure 2c) when compared to disease control or vehicle treated PH rats. Cardiac echo analysis of PAT/pulmonary ejection time (PET) ratio (Figure 2d) and tricuspid valve regurgitation (TVR) (Figure 2e) suggest a reduction of pulmonary artery back-pressure with the potential to restore diastolic function. We next analysed the mid-systolic decrease in PA flow velocity in the PA flow-time-curves, known as the 'notch' in rat models of PH. Notch duration has previously been reported and linked to PH disease severity [32]. We report a correlation between notch duration and pulmonary arterial pressure (emPAP) (Supplemental-Figure 5c) with PT2567 intervention

decreasing notch duration when compared to vehicle treated rats (Supplemental-Figure 5d-e).

PVR is coupled to both pulmonary pressure and CO and is thought to better reflect the pathophysiology of PH as it, to a large extent, is a result of vascular remodelling in peripheral vessels. PVR was calculated by both catheterisation (estimation Pulmonary Vascular Resistance index = EmPAP – endDP / Ci)[33] and cardiac echo (Woods index WU = 10 X TVR / $RVOT_{VTI}$)(additional parameters used in PVR calculation are shown in Supplemental-Figure 5f-i). PT2567 intervention significantly reduced ePVRi (1.486±0.59, $p<0.05$) and Woods index (1.167±0.615, $p<0.05$) when compared to vehicle control (2.605±1.370 and 1.897±0.783, respectively) (Figure 2f-g). HIF2α inhibition also restored $RVOT_{VTI}$ to values similar to normoxic vehicle controls (Supplemental-Figure 5j), while all other su5416/hypoxia treated groups maintained substantially lower $RVOT_{VTI.}$ Left heart blood pressure and heart rate were unaffected by either PT2567 or sildenafil when compared to normoxic vehicle control (Supplemental-Figure 5k-l). Of note, normoxic-vehicle and normoxic-PT2567 groups did not show any difference across all haemodynamic analyses.

PT2567 intervention reduces pulmonary vascular remodelling

We next evaluated serial histological sections of inflated lungs for vascular remodelling. Lung sections were stained with Verhoeffs Van Gieson (elastic tissue fibre) (figure 3a), von-Willebrand factor, and immunostained for αSMA, Ki67 (cell proliferation marker)(Figure 3e) and myeloperoxidase (MPO) (Supplemental-Figure 6g- h). Pulmonary histopathology scoring is presented in supplemental table 1b. The incidence of smooth muscle hypertrophy, perivascular/vascular inflammation and perivascular fibrosis was decreased in both PT2567 and Sildenafil intervention groups when compared to su5416/hypoxia-vehicle group. Group mean scores for smooth muscle hypertrophy, perivascular/vascular inflammation and fibrosis were 0.66, 5.70, 8.90, 4.70 and 5.90 in normoxia vehicle, su5416/hypoxia, su5416/hypoxia-vehicle, su5416/hypoxia-PT2567 100mg/kg, and su5416/hypoxia-sildenafil, respectively.

We also assessed medial thickening in the larger bronchial associated pulmonary vessels as a measure of neointimal lesions.. Rats exposed to su5416/hypoxia for 3 weeks showed a significant increase in medial thickness compared to normoxic vehicle controls with further remodelling noted in su5416/hypoxia-vehicle (Figure 3b). In comparison, both PT2567 and sildenafil intervention demonstrated a significant reduction in medial thickness relative to su5416/hypoxia-vehicle (Figure 3b). Next, we assessed the extent of small arterial occlusion. Vessels (≥50μm) were determined to be either fully occluded or with an open lumen. PT2567 and Sildenafil intervention significantly reduced the degree of vessel occlusion when compared to su5416/hypoxia or su5416/hypoxia-vehicle (Figure 3c). Furthermore, lung sections from su5416/hypoxia-vehicle showed an increase in elastin and αSMA associated with pulmonary vessels (Figure 3e, Supplemental-Figure 6a). This was partially inhibited by PT2567 intervention, with a substantial reduction in αSMA deposition in distal vessels, particularly of fully muscularised vessels compared to the su5416/hypoxia-vehicle group (Figure 3d, Supplemental-Figure 6b-d). Quantification of the expression of markers of proliferation (Ki67) further confirmed that both PT2567 and Sildenafil reduced su5426/hypoxia-induced pulmonary vessel proliferation (Supplemental-Figure 6e) and, more specifically, PAEC proliferation (Supplemental-Figure 6f). Finally, quantification of MPO in lung sections revealed reduced immunoreactivity in perivascular regions of rats treated with PT2567 when compared to su5426/hypoxia-3w and su5426/hypoxia-vehicle animals, with no change in MPO immunoreactivity in intravascular regions (Supplemental-Figure 6g-h).

Taken together, these data suggest that inhibition of HIF2α function with PT2567 reduces pulmonary vascular remodelling and the dynamic changes in cardiovascular function associated with this PH model.

PT2567 modulates PH associated gene expression and normalises plasma nitrite levels

Having identified a difference in pulmonary vascular remodelling with PT2567, we next investigated the pulmonary expression profiles of known HIFα target genes associated with

glycolysis, inflammation and pulmonary remodelling in whole lung samples. Relatively little is known about the global inhibition of HIF2α and effects on the multicellular componentry of the lung in PH models. Given the systemic administration of PT2567 it was thought advantageous to analyse the whole lung. PT2567 intervention normalised the expression of known HIF2α target genes, *glut1* and *ca9* when compared to su5416/hypoxia-vehicle control (Supplemental-Figure 7a-b), with little effect on HIF1α target gene expression, *ldha* and pgk1 (Supplemental-Figure 7c-d). Su5416/hypoxia significantly increased the gene expression of inflammatory targets *cxcl12* and receptor *cxcr4,* and endothelial adhesion molecules *icam1* and *sele.* PT2567 intervention reduced gene expression to near normoxia non-disease animals (Supplemental-Figure 7e-h). Next, we analysed signalling targets associated with PH, including *apln*, *arg2*, cell-cycle *ccnd1*, *pai1*, vaso-active *edn-1* were all reduced and *id1* expression restored following PT2567 intervention (Supplemental-Figure 7i-n). Sildenafil normalised the expression of *glut1, cxcl12* and *id1* but did not impact on the expression of any other genes.

Given that PAH pathophysiology increases RVH that often ends in right-heart failure and death, we next investigated the expression of structural and stress associated genes in RV tissues. PT2567 significantly reduced the expression of myosin heavy chain-7 (*myh7*) and actin-alpha-1 (*acta1*) and myosin light chain-3 (*myl3*) trended towards normal expression (p=0.065 non-parametric analysis) when compared with su5416/hypoxia-vehicle treated rats (Supplemental-Figure 8a-c). The cardiac stress genes natriuretic peptide A (*nppa*), natriuretic peptide B (*nppb*) and annexin A5 (*anxa5*) and the fibrosis targets collagen type-1 A1 (*col1a1*) type-3 a1 (*col3a1*) and tissue inhibitor of metalloproteinase 2 (*timp2*) were reduced following PT2567 intervention (Supplemental-Figure 8d-i), sildenafil only reduced the expression of *col3a1* and *timp2* .

Next we analysed plasma samples for cytokines, markers of cardiac stress and nitrites in the su5416/hypoxia rat model. PT2567 intervention significantly reduced plasma TNFα concentration (Figure 4a) and increased immuno-suppressive IL-10 (Figure 4b) when

compared to su5416/hypoxia-vehicle rats. Other plasma cytokines including IL-13, IL-4, IL-5, IFN-γ, IL-1β and IL-8 were also measured (Table 2) but did not reach significance when compared to su5416/hypoxia-vehicle control.

Table 2 Plasma cytokine analysis

	IFN-γ (pg/ml)	IL-5 (pg/ml)	IL-1β (LOD 12pg/ml)	IL-8 (pg/ml)
Nx-Veh	4.45±0.68	19.26±2.61	12.31±0.62	40.70±5.57
SuHx 3-weeks	5.28±1.70	24.55±4.37	12.60±0.42	44.83±5.66
SuHx-Veh	6.43±0.96	26.77±4.90	14.05±0.91	51.19±4.18
SuHx-PT2567	9.90±1.62	21.44±2.46	12.49±0.47	48.44±4.30
SuHx-Sil	5.36±1.10	25.42±2.65	12.41±0.31	53.95±7.82

	IL-4 (LOD 2pg/ml)	IL-13 (pg/ml)
Nx-Veh	3.83±0.88	4.53±0.23
SuHx 3-weeks	3.36±0.89	5.67±0.91
SuHx-Veh	3.68±0.53	6.45±0.75
SuHx-PT2567	5.21±0.79*	8.46±0.94*
SuHx-Sil	2.26±0.20	4.35±0.15

We also noted the normalisation of plasma cardiac stress markers c-Troponin-I (c-TnI) and fatty acid binding protein-3 (FABP3) in the PT2567 treated group when compared to su5416/hypoxia-vehicle (Figure 4c-d).

Consistent with PH disease severity, we observed a significant decrease in plasma nitrites in su5416/hypoxia-vehicle (1.121±0.414) when compared to normoxia-vehicle (1.889±0.404μM). Notably, both PT2567 and sildenafil restored plasma nitrite concentrations to near normoxia-vehicle control levels (1.756±0.294 and 1.798±0.795 respectively) (Figure 4e).

PT2567 modulated blood counts within normal physiological limits

Whole blood analysis showed no change in white cell count. However, PT2567 treatment reduced red blood cell count, haemoglobin levels and percentage haematocrit towards the

lower reference value within the physiological range. However, these readings were not significantly different to vehicle control (Supplemental-Figure 9a-d).

Carotid body size is not affected during PT2567 intervention

Recent studies have shown that HIF2α is essential for carotid body (CB) development and growth in response to chronic hypoxia[34, 35]. Given the importance of the CB in regulating cardiorespiratory responses to hypoxia, we sought to determine whether PT2567 treatment impacted CB morphology and by extension its function. Histological analysis of carotid bifurcations from rats exposed to su5416/hypoxia for 3 weeks showed a significant increase in CB volume compared to Nx-control rats (Supplemental-Figure 10a, b and f). Typical CB shrinking across the re-oxygenation period was unaffected in both PT2567 or sildenafil treated rats compared to vehicle control group (Supplemental-Figure 10c-f).

PT2567 intervention increases survival rate in monocrotaline challenged rats

We also investigated the effect of PT2567 intervention in the MCT rat model of PH. As illustrated in Supplemental-Figure 11a, fourteen days after MCT challenge the rats received intervention with vehicle, PT2567 (100mg/kg) or sildenafil (30mg/kg) for two weeks. Cardiac echo was recorded 14 days following MCT challenge and at the end point of the intervention study (28 days). PT2567 intervention resulted in a 90% survival rate compared to 77% for sildenafil treated animals (Supplemental Figure 11b). Cardiac echo showed that PT2567 intervention offered a degree of protection for PAT/PET (ratio), RVOT-vti and cardiac output (Supplemental Figure 11c-e) when compared to vehicle treated animals. Sildenafil treated animals were not significantly different to vehicle treated animals across all cardiac echo parameters.

Inhibition of HIF2α normalises PAH patient-derived BOEC proliferation and arginase activity

BOECs have been extensively characterised and used as a model for studying *in vitro* endothelial function in vascular disorders[36, 37]. The BOECs used in this study were

previously characterised by flow cytometry immunostaining for CD133, CD34, VEGFR2 [36] and gene-array analysis that demonstrated their close functional and gene expression similarity to pulmonary artery endothelial cells[38]. Additionally, we previously demonstrated that these cells had no deficiencies in HIFα expression or hypoxic induced stability of these transcription factors.[16]

First, we evaluated the activity and specificity of PT2567 (1μM) in the aforementioned BOECs isolated from PAH patients and healthy volunteers. Human qPCR primers were selected to complement the analysis of rat whole lung gene expression used in the su5416/hypoxia model.

Hypoxic exposure of BOECs from healthy volunteers and PAH patients increased both HIF1α and HIF2α target genes (Figure 5a-g) consistent with our previous study. We also reported that hypoxia induced increase in *GLUT1*, *VEGF* and *ARG2* expression were greater in PAH BOECs when compared to control BOECs. Treatment with PT2567 markedly reduced hypoxia-induced *GLUT1*, *PAI-1*, *VEGF*, and *ARG2* expression without effecting HIF1α target gene transcripts *LDHA, PGK1* and *PDK1* in both control and PAH BOECs (Figure 5a-g).

Hyper-proliferation is a documented phenotype of BOECs isolated from PAH patient[36]. We initially utilised a short-hairpin knock-down strategy for HIF1α or HIF2α in control BOECs to initially assess the impact of these transcription factors on proliferation. shRNA-HIF2α substantially reduced cell proliferation in control BOEC on days 2-4 when compared to shRNA-Scramble, whereas shRNA-HIF1α had little/no effect on proliferation (Figure 5h). We next investigated the effect of PT2567 on BOEC proliferation. As previously documented, BOECs from PAH patients demonstrated a considerably higher rate of proliferation by day 4 and maintained to day 6 when compared to BOECs from healthy volunteers. Treatment with PT2567 reduced cell proliferation from both PAH patient and healthy volunteer derived BOECs (Figure 5i) without affecting the rate of cellular apoptosis as determined by caspase-3/7 activity (Figure 5j).

We have previously documented the aberrant expression and activity of arginase-2 in BOECs isolated from PAH patients[16] (human PAEC do not express arginase-1). Treatment with PT2567 for 24hrs suppressed arginase-2 enzyme activity in BOEC from PAH patients and healthy volunteers (Figure 5k). Taken together, these data demonstrate that targeting of HIF2α in BOECs derived from PAH patients, reduced aberrant HIF2α target genes expression and reduced the hyper-proliferative endothelial phenotype and arginase-2 activity to near healthy controls. Finally, we assessed the impact of PT2567 on BOECs network formation function. BOECs networks from PAH patients have been documented to be more fragile with shorter connections and smaller loops when compared to controls[36]. This network phenotype is partially corrected following PT2567 treatment by increasing both tube length (Supplemental-Figure 11a) and loop size (Supplemental-Figure 11b) to values similar as control BOECs. Representative photomicrographs of BOEC network formation following vehicle or PT2567 (1μM) treatment in healthy control BOEC (Supplemental-Figure 11c) and PAH BOEC (Supplemental-Figure 11d) are shown.

Discussion

In this study we have shown that HIF2α signalling is a key element in the development of PH and that specifically targeting this process with a novel global HIF2α inhibitor (PT2567) during the initiation phase (Figure 1) or as an intervention strategy (Figure 2) alleviated many of the pathologies, associated with PH disease.

The HIF2α inhibitor, PT2567, used throughout this study directly binds to a region within the PAS-B domain of HIF2α and disrupts the formation of HIF2α/ARNT dimer, a key event essential for HIF2α activation. Our *in vitro* studies confirmed the high affinity and specificity of PT2567 for HIF2α and the low micro-molar concentration required for HIF2α target gene inhibition. We also report that HIF2α signalling is potentially involved in the hyper-proliferative and endothelial network phenotype observed in BOECs derived from PAH patient via the expression of HIF2α target genes (*GLUT1*, *VEGF*, *PAI2* and *ARG2*).

Our *in vivo* pharmokinetic analysis identified a favourable oral bioavailability and plasma stability profile in adult rodents (supplemental figure 1-4) at concentrations subsequently used in both prevention and intervention protocols. The su5416/hypoxia prevention protocol confirmed several key observations previously described in murine HIF2α manipulation models of PH, but also further established that inhibition of global HIF2α activity directly influenced PH disease initiation. PT2567 intervention reduced pulmonary vascular resistance, vascular remodelling and increased cardiac function in the su5416/hypoxia model, and offered a significant survival advantage in the monocrotaline PH model. Sildenafil was used as a clinical comparative throughout these studies, but offered only a small beneficial effect in both prevention and intervention studies. We think this discrepancy is probably due to the timing of the haemodynamic analysis, being completed 16-18hrs after the final dose and therefore potentially outside of the vasoactive window.

Although increased HIF2α protein stability has been identified in pulmonary vascular occlusive lesions from both IPAH patients and rodent PH models, the mechanistic role of HIF2α in the initiation and progression of PH remains unclear. The vast majority of published *in vivo* studies that question a role for HIFα in the initiation and development of PH use tissue-specific gene deletion mouse models. Although these tissue-specific mouse models are incredibly useful to determine gene contribution in disease development, they do not take account of potential developmental shortcomings that may influence normal physiological or pathological responses, and how specific gene function may differ across multiple vascular beds to influence disease progression or severity.

The primary goal of this study was to determine the impact of global HIF2α inhibition in preventing and reverting pulmonary hypertension and to investigate the pathological influence of this transcription factor in regulating the expression of potential PH associated target genes that systematically influence vascular homeostasis.

To this end, we investigated the gene expression profiles in whole lung samples from our rodent PH models to ensure the inclusion of all pulmonary cell types necessary for PH

disease progression. These data confirmed the specificity of PT2567, and showed reduced expression of inflammatory (*cxcl12, cxcr4, icam1, sele*) and signalling targets (*apln, arg2, ccnd1, pai1 and edn1*) associated with PH with the additional restoration of *id1 gene expression*. Although the impact of sildenafil treatment on haemodynamic parameters appeared less impressive in these animals studied, the influence of sildenafil on whole lung gene expression patterns was not dissimilar to PT2567. Further studies with concomitant or alternate PT2567 and sildenafil treatment may be clinically relevant.

Recent studies by Dai *et al*[39] and Hu and colleagues [40] offers further support for the important role of HIF2α in PH and confirmed many of these inflammatory and signalling target genes. Furthermore, Hu *et al* utilised PT2567 in a hypobaric hypoxic rat model of PH and reported a reduction in both pulmonary arterial pressures and vascular remodelling[40]. In line with this, our study confirmed a reduction in pulmonary vascular smooth muscle deposition and also shows a reduction in pulmonary vascular endothelial cell proliferation and MPO+ve cells (myeloid-lineage) in the perivascular regions.

These finding are also consistent with those previously published using murine tissue-type specific HIF2α deletion models, reporting a reduction in endothelial vasoactive function (*edn1, arg-2, apln*)[8, 9, 16], cellular proliferation/ angiogenesis (*ccnd1, vegf*)[16], and endothelial-to-mesenchymal transition (*snai1/2*) targets[41].

We previously documented that deletion of pulmonary endothelial HIF2α reduced circulating pro-inflammatory cytokines and growth factors (IL-6, IL-8, TNFα, IL-1β Cxcl12) in the chronic-hypoxia PH model.[16] High circulating concentrations of these factors are associated with poor PAH patient prognosis[42]. We report that PT2567 intervention reduced circulating TNFα and increased immune-suppressive IL-10 plasma concentrations. A previous report described the administration of recombinant IL-10 to MCT challenged rats reduced haemodynamics and pulmonary vascular remodelling and provided a survival advantage over vehicle control.[43] Other murine inflammatory models have linked aberrant myeloid HIF2α expression with low plasma IL-10 concentrations, where mice deficient in

myeloid-HIF2α restored/increased plasma IL-10.[44] Further investigations would be required to clarify the cellular source (Tregs, macrophages, B-cells, dendritic cells) and role of HIFα modulation of IL-10 in PAH.

The circulating concentration of nitric oxide (NO) is key to the structural integrity and function of the cardiovascular system. Reduced NO bioavailability is associated with endothelial dysfunction, smooth muscle proliferation, and with implications in the development of cardiovascular and PAH disease severity[45-48]. We show here that plasma NO/nitrite concentrations are restored to near normal/normoxia values following intervention with PT2567 or sildenafil. These data are consistent with those of our previous investigations in the murine chronic-hypoxia PH model[16], where we described a HIF2α-Arg2 axis as essential for the development of PH. We showed that increased arginase expression and activity led to dysregulation of vascular NO homeostasis.[16] Sildenafil indirectly modulates endothelial function via endothelial nitric oxide synthesis[49] in models of PH. However, the action of sildenafil on plasma nitrite is thought to be independent of HIF signalling

Given the global HIF2α inhibition of PT2567, other non-pulmonary tissues may also indirectly modulate PH disease progression. We report that PT2567 intervention reduces the expression of several RV genes associated with structural and stress induced adaptation, however based on what little is known about HIF2α signalling in cardiovascular disease we cannot fully differentiate restoration of cardiac function as a direct effect of PT2567 or indirectly as a result of pulmonary vascular function.

The role of HIF1α in the initiation and development of PH remains controversial. The lack of specific HIF1α inhibitors hampers potential intervention studies in the rat su5416/hypoxia or monocrotaline models. Therefore, the vast majority of the studies used tissue-specific knockout mouse models that demonstrated variable outcomes depending on the tissues targeted and the methodology used to aberrantly activate (PHD or VHL) or inhibit HIF1α

stability. Targeting HIF1α signalling in smooth muscle cells has shown, to some extent, a beneficial effect in slowing down the progression of the disease[50]. We previously investigated the role of pulmonary endothelial HIF1α in a chronic hypoxia murine model of PH. We did not observe a difference in PH disease development over a 7-14-21 day hypoxic time course when compared to wild-type animals. Furthermore, Hu et al recently reported that global inhibition of HIF1α in a chronic hypoxic model of PH did not support a central role for this transcription factor in PH development. Further investigations are required to clarify if HIF1α or the combination of HIF1α/HIF2α influences the development of PH.

The current consensus view supports a role for HIF2α in the development of PAH, most probably through influencing multiple signalling pathways across pulmonary vascular beds leading to the progressive loss of vascular identity/plasticity/homeostasis that drives remodelling and increases vessel resistance. The degree of protection offered by PT2567 intervention in this manuscript may be attributed, to some extent, to the modulation of multiple PH associated target genes for *glut1, cxcl12, apln, edn1, icam1, sele* and *ccnd1* in pulmonary tissues, although contributions from other known PAH targets including *bmpr2*[26], *il-6*[51], *sox17*[52], *cav1*[53] across multiple tissues and other organs are most probable and cannot be ruled out.

The roles played by aberrant HIF2α stability and function in the development of PH has been an area of intense interest for nearly two decades[8, 9, 12, 16, 54, 55]. These collective studies clearly elucidate a pivotal role of vascular HIF2α in PH disease initiation and progression and support its evaluation as a novel therapeutic target for the treatment of PH patients. However, unlike the uniform genetic background of *in vivo* murine models used to establish genetic targets, PAH is a complex dynamic disease characterised by considerable patient heterogeneity. Thus, further investigations will be needed to determine the overall sensitivity of PAH population to HIF2α inhibitors and also clarify the combination effect of PT2567 with current therapeutic strategies. We believe the current organ-on-a-chip

technology combined with blood outgrowth endothelial cells from PAH patients could provide an excellent platform to further characterise the role of HIF2α in PH.

In conclusion, our work provides a greater understanding of direct inhibition of HIF2α transcriptional activity in PH initiation and progression in the su5416/hypoxia rodent model of PH. Further research is required to determine the position of HIF2α in the hierarchy of factors required to initiate PH and how prolonged HIF2α inhibition impacts not only on PH disease pathology but also in other essential physiological processes.

Acknowledgements:

Author contribution: D.M., S.M., X.D., H.T., E.M.W., and A,S.C., designed research; D.M., S.M., A.C., M.S., A.V., A.J.T.W., X.D., H.T., and A,S.C performed research; D.M., S.M., and A.S.C., analysed data; and D.M., E.M.W., and A.S.C. wrote the paper

Sources of Funding: National Institute for Health Research Cambridge Biomedical Research Centre, Peloton Therapeutics Inc.

Disclosures: Peloton Therapeutics Inc provided funding for this study.

Nonstandard Abbreviations and Acronyms

PAH pulmonary arterial hypertension

HIF hypoxia inducible factor

CO cardiac output

PA pulmonary artery

TVR tricuspid valve regurgitation

PAT pulmonary artery acceleration time

PET pulmonary artery ejection time

emPAP estimation of pulmonary artery pressure

Ci Cardiac index

ePVRi estimation of pulmonary vascular resistance index

RVSP right ventricle systolic pressure

endDP end diastolic pressure

$RVOT_{vti}$ right ventricle outflow tract-velocity time integral

hPAEC human pulmonary artery endothelial cells

CH chronic hypoxia

RV right ventricle

PVR pulmonary vascular resistance

RVH right ventricle hypertrophy

PHD prolyl-hydroxylase

Su Sugen 5416

Hx hypoxia

Nx normoxia

ARNT aryl hydrocarbon receptor nuclear translocator

ccRCC clear cell renal cell carcinoma

1. von Euler US, Liljestrand, G. Observations on the pulmonary arterial blood pressure in the cat. *Acta Physiologica Scand* 1946: 12: 19.

2. Lettieri CJ, Nathan SD, Barnett SD, Ahmad S, Shorr AF. Prevalence and outcomes of pulmonary arterial hypertension in advanced idiopathic pulmonary fibrosis. *Chest* 2006: 129(3): 746-752.

3. Naeije R. Pulmonary hypertension and right heart failure in chronic obstructive pulmonary disease. *Proc Am Thorac Soc* 2005: 2(1): 20-22.

4. Sylvester JT, Shimoda LA, Aaronson PI, Ward JP. Hypoxic pulmonary vasoconstriction. *Physiol Rev* 2012: 92(1): 367-520.

5. Semenza GL, Shimoda LA, Prabhakar NR. Regulation of gene expression by HIF-1. *Novartis Found Symp* 2006: 272: 2-8; discussion 8-14, 33-16.

6. Takeda N, O'Dea EL, Doedens A, Kim JW, Weidemann A, Stockmann C, Asagiri M, Simon MC, Hoffmann A, Johnson RS. Differential activation and antagonistic function of HIF-{alpha} isoforms in macrophages are essential for NO homeostasis. *Genes Dev* 2010: 24(5): 491-501.

7. Tyrakis PA, Palazon A, Macias D, Lee KL, Phan AT, Velica P, You J, Chia GS, Sim J, Doedens A, Abelanet A, Evans CE, Griffiths JR, Poellinger L, Goldrath AW, Johnson RS. S-2-hydroxyglutarate regulates CD8(+) T-lymphocyte fate. *Nature* 2016: 540(7632): 236-241.

8. Dai Z, Li M, Wharton J, Zhu MM, Zhao YY. Prolyl-4 Hydroxylase 2 (PHD2) Deficiency in Endothelial Cells and Hematopoietic Cells Induces Obliterative Vascular Remodeling and Severe Pulmonary Arterial Hypertension in Mice and Humans Through Hypoxia-Inducible Factor-2alpha. *Circulation* 2016: 133(24): 2447-2458.

9. Kapitsinou PP, Rajendran G, Astleford L, Michael M, Schonfeld MP, Fields T, Shay S, French JL, West J, Haase VH. The Endothelial Prolyl-4-Hydroxylase Domain 2/Hypoxia-Inducible Factor 2 Axis Regulates Pulmonary Artery Pressure in Mice. *Mol Cell Biol* 2016: 36(10): 1584-1594.

10. Boucherat O, Vitry G, Trinh I, Paulin R, Provencher S, Bonnet S. The cancer theory of pulmonary arterial hypertension. *Pulm Circ* 2017: 7(2): 285-299.

11. Bonnet S, Michelakis ED, Porter CJ, Andrade-Navarro MA, Thebaud B, Bonnet S, Haromy A, Harry G, Moudgil R, McMurtry MS, Weir EK, Archer SL. An abnormal mitochondrial-hypoxia inducible factor-1alpha-Kv channel pathway disrupts oxygen sensing and triggers pulmonary arterial hypertension in fawn hooded rats: similarities to human pulmonary arterial hypertension. *Circulation* 2006: 113(22): 2630-2641.

12. Shimoda LA, Manalo DJ, Sham JS, Semenza GL, Sylvester JT. Partial HIF-1alpha deficiency impairs pulmonary arterial myocyte electrophysiological responses to hypoxia. *Am J Physiol Lung Cell Mol Physiol* 2001: 281(1): L202-208.

13. Brusselmans K, Compernolle V, Tjwa M, Wiesener MS, Maxwell PH, Collen D, Carmeliet P. Heterozygous deficiency of hypoxia-inducible factor-2alpha protects mice against pulmonary hypertension and right ventricular dysfunction during prolonged hypoxia. *J Clin Invest* 2003: 111(10): 1519-1527.

14. Ball MK, Waypa GB, Mungai PT, Nielsen JM, Czech L, Dudley VJ, Beussink L, Dettman RW, Berkelhamer SK, Steinhorn RH, Shah SJ, Schumacker PT. Regulation of hypoxia-induced pulmonary hypertension by vascular smooth muscle hypoxia-inducible factor-1alpha. *Am J Respir Crit Care Med* 2014: 189(3): 314-324.

15. Barnes EA, Chen CH, Sedan O, Cornfield DN. Loss of smooth muscle cell hypoxia inducible factor-1alpha underlies increased vascular contractility in pulmonary hypertension. *FASEB J* 2017: 31(2): 650-662.

16. Cowburn AS, Crosby A, Macias D, Branco C, Colaco RD, Southwood M, Toshner M, Crotty Alexander LE, Morrell NW, Chilvers ER, Johnson RS. HIF2alpha-arginase axis is essential for the development of pulmonary hypertension. *Proc Natl Acad Sci U S A* 2016: 113(31): 8801-8806.

17. Formenti F, Beer PA, Croft QP, Dorrington KL, Gale DP, Lappin TR, Lucas GS, Maher ER, Maxwell PH, McMullin MF, O'Connor DF, Percy MJ, Pugh CW, Ratcliffe PJ, Smith TG, Talbot NP, Robbins PA. Cardiopulmonary function in two human disorders of the hypoxia-inducible factor (HIF) pathway: von Hippel-Lindau disease and HIF-2alpha gain-of-function mutation. *FASEB J* 2011: 25(6): 2001-2011.

18. Tan Q, Kerestes H, Percy MJ, Pietrofesa R, Chen L, Khurana TS, Christofidou-Solomidou M, Lappin TR, Lee FS. Erythrocytosis and pulmonary hypertension in a mouse model of human HIF2A gain of function mutation. *J Biol Chem* 2013: 288(24): 17134-17144.

19. Scheuermann TH, Tomchick DR, Machius M, Guo Y, Bruick RK, Gardner KH. Artificial ligand binding within the HIF2alpha PAS-B domain of the HIF2 transcription factor. *Proc Natl Acad Sci U S A* 2009: 106(2): 450-455.

20. Zimmer M, Ebert BL, Neil C, Brenner K, Papaioannou I, Melas A, Tolliday N, Lamb J, Pantopoulos K, Golub T, Iliopoulos O. Small-molecule inhibitors of HIF-2a translation link its 5'UTR iron-responsive element to oxygen sensing. *Mol Cell* 2008: 32(6): 838-848.

21. Chen W, Hill H, Christie A, Kim MS, Holloman E, Pavia-Jimenez A, Homayoun F, Ma Y, Patel N, Yell P, Hao G, Yousuf Q, Joyce A, Pedrosa I, Geiger H, Zhang H, Chang J, Gardner KH, Bruick RK, Reeves C, Hwang TH, Courtney K, Frenkel E, Sun X, Zojwalla N, Wong T, Rizzi JP, Wallace EM, Josey JA, Xie Y, Xie XJ, Kapur P, McKay RM, Brugarolas J. Targeting renal cell carcinoma with a HIF-2 antagonist. *Nature* 2016: 539(7627): 112-117.

22. Cho H, Du X, Rizzi JP, Liberzon E, Chakraborty AA, Gao W, Carvo I, Signoretti S, Bruick RK, Josey JA, Wallace EM, Kaelin WG. On-target efficacy of a HIF-2alpha antagonist in preclinical kidney cancer models. *Nature* 2016: 539(7627): 107-111.

23. Courtney KD, Infante JR, Lam ET, Figlin RA, Rini BI, Brugarolas J, Zojwalla NJ, Lowe AM, Wang K, Wallace EM, Josey JA, Choueiri TK. Phase I Dose-Escalation Trial of PT2385, a First-in-Class Hypoxia-Inducible Factor-2alpha Antagonist in Patients With Previously Treated Advanced Clear Cell Renal Cell Carcinoma. *J Clin Oncol* 2018: 36(9): 867-874.

24. Wallace EM, Rizzi JP, Han G, Wehn PM, Cao Z, Du X, Cheng T, Czerwinski RM, Dixon DD, Goggin BS, Grina JA, Halfmann MM, Maddie MA, Olive SR, Schlachter ST, Tan H, Wang B, Wang K, Xie S, Xu R, Yang H, Josey JA. A Small-Molecule Antagonist of HIF2alpha Is Efficacious in Preclinical Models of Renal Cell Carcinoma. *Cancer Res* 2016: 76(18): 5491-5500.

25. Wehn PM, Rizzi JP, Dixon DD, Grina JA, Schlachter ST, Wang B, Xu R, Yang H, Du X, Han G, Wang K, Cao Z, Cheng T, Czerwinski RM, Goggin BS, Huang H, Halfmann MM, Maddie MA, Morton EL, Olive SR, Tan H, Xie S, Wong T, Josey JA, Wallace EM. Design and Activity of Specific Hypoxia-Inducible Factor-2alpha (HIF-2alpha) Inhibitors for the Treatment of Clear Cell Renal Cell Carcinoma: Discovery of Clinical Candidate (S)-3-((2,2-Difluoro-1-hydroxy-7-(methylsulfonyl)-2,3-dihydro-1 H-inden-4-yl)oxy)-5-fluorobenzonitrile (PT2385). *J Med Chem* 2018: 61(21): 9691-9721.

26. Long L, Ormiston ML, Yang X, Southwood M, Graf S, Machado RD, Mueller M, Kinzel B, Yung LM, Wilkinson JM, Moore SD, Drake KM, Aldred MA, Yu PB, Upton PD, Morrell NW. Selective enhancement of endothelial BMPR-II with BMP9 reverses pulmonary arterial hypertension. *Nat Med* 2015: 21(7): 777-785.

27. Crosby A, Soon E, Jones FM, Southwood MR, Haghighat L, Toshner MR, Raine T, Horan I, Yang P, Moore S, Ferrer E, Wright P, Ormiston ML, White RJ, Haight DA, Dunne DW, Morrell NW. Hepatic Shunting of Eggs and Pulmonary Vascular Remodeling in Bmpr2(+/-) Mice with Schistosomiasis. *Am J Respir Crit Care Med* 2015: 192(11): 1355-1365.

28. Morrell NW, Atochina EN, Morris KG, Danilov SM, Stenmark KR. Angiotensin converting enzyme expression is increased in small pulmonary arteries of rats with hypoxia-induced pulmonary hypertension. *J Clin Invest* 1995: 96(4): 1823-1833.

29. Schindelin J, Arganda-Carreras I, Frise E, Kaynig V, Longair M, Pietzsch T, Preibisch S, Rueden C, Saalfeld S, Schmid B, Tinevez JY, White DJ, Hartenstein V, Eliceiri K, Tomancak P, Cardona A. Fiji: an open-source platform for biological-image analysis. *Nat Methods* 2012: 9(7): 676-682.

30. Macias D, Fernandez-Aguera MC, Bonilla-Henao V, Lopez-Barneo J. Deletion of the von Hippel-Lindau gene causes sympathoadrenal cell death and impairs chemoreceptor-mediated adaptation to hypoxia. *EMBO Mol Med* 2014: 6(12): 1577-1592.

31. Zhang C, Hein TW, Wang W, Miller MW, Fossum TW, McDonald MM, Humphrey JD, Kuo L. Upregulation of vascular arginase in hypertension decreases nitric oxide-mediated dilation of coronary arterioles. *Hypertension* 2004: 44(6): 935-943.

32. Urboniene D, Haber I, Fang YH, Thenappan T, Archer SL. Validation of high-resolution echocardiography and magnetic resonance imaging vs. high-fidelity catheterization in experimental pulmonary hypertension. *Am J Physiol Lung Cell Mol Physiol* 2010: 299(3): L401-412.

33. Hameed AG, Arnold ND, Chamberlain J, Pickworth JA, Paiva C, Dawson S, Cross S, Long L, Zhao L, Morrell NW, Crossman DC, Newman CM, Kiely DG, Francis

SE, Lawrie A. Inhibition of tumor necrosis factor-related apoptosis-inducing ligand (TRAIL) reverses experimental pulmonary hypertension. *J Exp Med* 2012: 209(11): 1919-1935.

34. Macias D, Cowburn AS, Torres-Torrelo H, Ortega-Saenz P, Lopez-Barneo J, Johnson RS. HIF-2alpha is essential for carotid body development and function. *Elife* 2018: 7.

35. Hodson EJ, Nicholls LG, Turner PJ, Llyr R, Fielding JW, Douglas G, Ratnayaka I, Robbins PA, Pugh CW, Buckler KJ, Ratcliffe PJ, Bishop T. Regulation of ventilatory sensitivity and carotid body proliferation in hypoxia by the PHD2/HIF-2 pathway. *J Physiol* 2016: 594(5): 1179-1195.

36. Toshner M, Voswinckel R, Southwood M, Al-Lamki R, Howard LS, Marchesan D, Yang J, Suntharalingam J, Soon E, Exley A, Stewart S, Hecker M, Zhu Z, Gehling U, Seeger W, Pepke-Zaba J, Morrell NW. Evidence of dysfunction of endothelial progenitors in pulmonary arterial hypertension. *Am J Respir Crit Care Med* 2009: 180(8): 780-787.

37. Wang JW, Bouwens EA, Pintao MC, Voorberg J, Safdar H, Valentijn KM, de Boer HC, Mertens K, Reitsma PH, Eikenboom J. Analysis of the storage and secretion of von Willebrand factor in blood outgrowth endothelial cells derived from patients with von Willebrand disease. *Blood* 2013: 121(14): 2762-2772.

38. Toshner M, Dunmore BJ, McKinney EF, Southwood M, Caruso P, Upton PD, Waters JP, Ormiston ML, Skepper JN, Nash G, Rana AA, Morrell NW. Transcript analysis reveals a specific HOX signature associated with positional identity of human endothelial cells. *PLoS One* 2014: 9(3): e91334.

39. Dai Z, Zhu MM, Peng Y, Machireddy N, Evans CE, Machado R, Zhang X, Zhao YY. Therapeutic Targeting of Vascular Remodeling and Right Heart Failure in Pulmonary Arterial Hypertension with a HIF-2alpha Inhibitor. *Am J Respir Crit Care Med* 2018: 198(11): 1423-1434.

40. Hu CJ, Poth JM, Zhang H, Flockton A, Laux A, Kumar S, McKeon B, Frid MG, Mouradian G, Li M, Riddle S, Pugliese SC, Brown RD, Wallace EM, Graham BB, Stenmark KR. Suppression of HIF2 signalling attenuates the initiation of hypoxia-induced pulmonary hypertension. *Eur Respir J* 2019.

41. Tang H, Babicheva A, McDermott KM, Gu Y, Ayon RJ, Song S, Wang Z, Gupta A, Zhou T, Sun X, Dash S, Wang Z, Balistrieri A, Zheng Q, Cordery AG, Desai AA, Rischard F, Khalpey Z, Wang J, Black SM, Garcia JGN, Makino A, Yuan JX. Endothelial HIF-2alpha contributes to severe pulmonary hypertension due to endothelial-to-mesenchymal transition. *Am J Physiol Lung Cell Mol Physiol* 2018: 314(2): L256-L275.

42. Groth A, Vrugt B, Brock M, Speich R, Ulrich S, Huber LC. Inflammatory cytokines in pulmonary hypertension. *Respir Res* 2014: 15: 47.

43. Ito T, Okada T, Miyashita H, Nomoto T, Nonaka-Sarukawa M, Uchibori R, Maeda Y, Urabe M, Mizukami H, Kume A, Takahashi M, Ikeda U, Shimada K, Ozawa

K. Interleukin-10 expression mediated by an adeno-associated virus vector prevents monocrotaline-induced pulmonary arterial hypertension in rats. *Circ Res* 2007: 101(7): 734-741.

44. Imtiyaz HZ, Williams EP, Hickey MM, Patel SA, Durham AC, Yuan LJ, Hammond R, Gimotty PA, Keith B, Simon MC. Hypoxia-inducible factor 2alpha regulates macrophage function in mouse models of acute and tumor inflammation. *J Clin Invest* 2010: 120(8): 2699-2714.

45. Klinger JR, Abman SH, Gladwin MT. Nitric oxide deficiency and endothelial dysfunction in pulmonary arterial hypertension. *Am J Respir Crit Care Med* 2013: 188(6): 639-646.

46. Klinger JR. Plasma nitrite/nitrate levels: a new biomarker for pulmonary arterial hypertension? *Eur Respir J* 2016: 48(5): 1265-1267.

47. Kleinbongard P, Dejam A, Lauer T, Jax T, Kerber S, Gharini P, Balzer J, Zotz RB, Scharf RE, Willers R, Schechter AN, Feelisch M, Kelm M. Plasma nitrite concentrations reflect the degree of endothelial dysfunction in humans. *Free Radic Biol Med* 2006: 40(2): 295-302.

48. Allen JD, Miller EM, Schwark E, Robbins JL, Duscha BD, Annex BH. Plasma nitrite response and arterial reactivity differentiate vascular health and performance. *Nitric Oxide* 2009: 20(4): 231-237.

49. Yin J, Kukucka M, Hoffmann J, Sterner-Kock A, Burhenne J, Haefeli WE, Kuppe H, Kuebler WM. Sildenafil preserves lung endothelial function and prevents pulmonary vascular remodeling in a rat model of diastolic heart failure. *Circ Heart Fail* 2011: 4(2): 198-206.

50. Yu AY, Shimoda LA, Iyer NV, Huso DL, Sun X, McWilliams R, Beaty T, Sham JS, Wiener CM, Sylvester JT, Semenza GL. Impaired physiological responses to chronic hypoxia in mice partially deficient for hypoxia-inducible factor 1alpha. *J Clin Invest* 1999: 103(5): 691-696.

51. Steiner MK, Syrkina OL, Kolliputi N, Mark EJ, Hales CA, Waxman AB. Interleukin-6 overexpression induces pulmonary hypertension. *Circ Res* 2009: 104(2): 236-244, 228p following 244.

52. Zhu N, Welch CL, Wang J, Allen PM, Gonzaga-Jauregui C, Ma L, King AK, Krishnan U, Rosenzweig EB, Ivy DD, Austin ED, Hamid R, Pauciulo MW, Lutz KA, Nichols WC, Reid JG, Overton JD, Baras A, Dewey FE, Shen Y, Chung WK. Rare variants in SOX17 are associated with pulmonary arterial hypertension with congenital heart disease. *Genome Med* 2018: 10(1): 56.

53. Zhao YY, Liu Y, Stan RV, Fan L, Gu Y, Dalton N, Chu PH, Peterson K, Ross J, Jr., Chien KR. Defects in caveolin-1 cause dilated cardiomyopathy and pulmonary hypertension in knockout mice. *Proc Natl Acad Sci U S A* 2002: 99(17): 11375-11380.

54. Shimoda LA, Semenza GL. HIF and the lung: role of hypoxia-inducible factors in pulmonary development and disease. *Am J Respir Crit Care Med* 2011: 183(2): 152-156.

55. Brusselmans K, Bono F, Maxwell P, Dor Y, Dewerchin M, Collen D, Herbert JM, Carmeliet P. Hypoxia-inducible factor-2alpha (HIF-2alpha) is involved in the apoptotic response to hypoglycemia but not to hypoxia. *J Biol Chem* 2001: 276(42): 39192-39196.

Figure 1

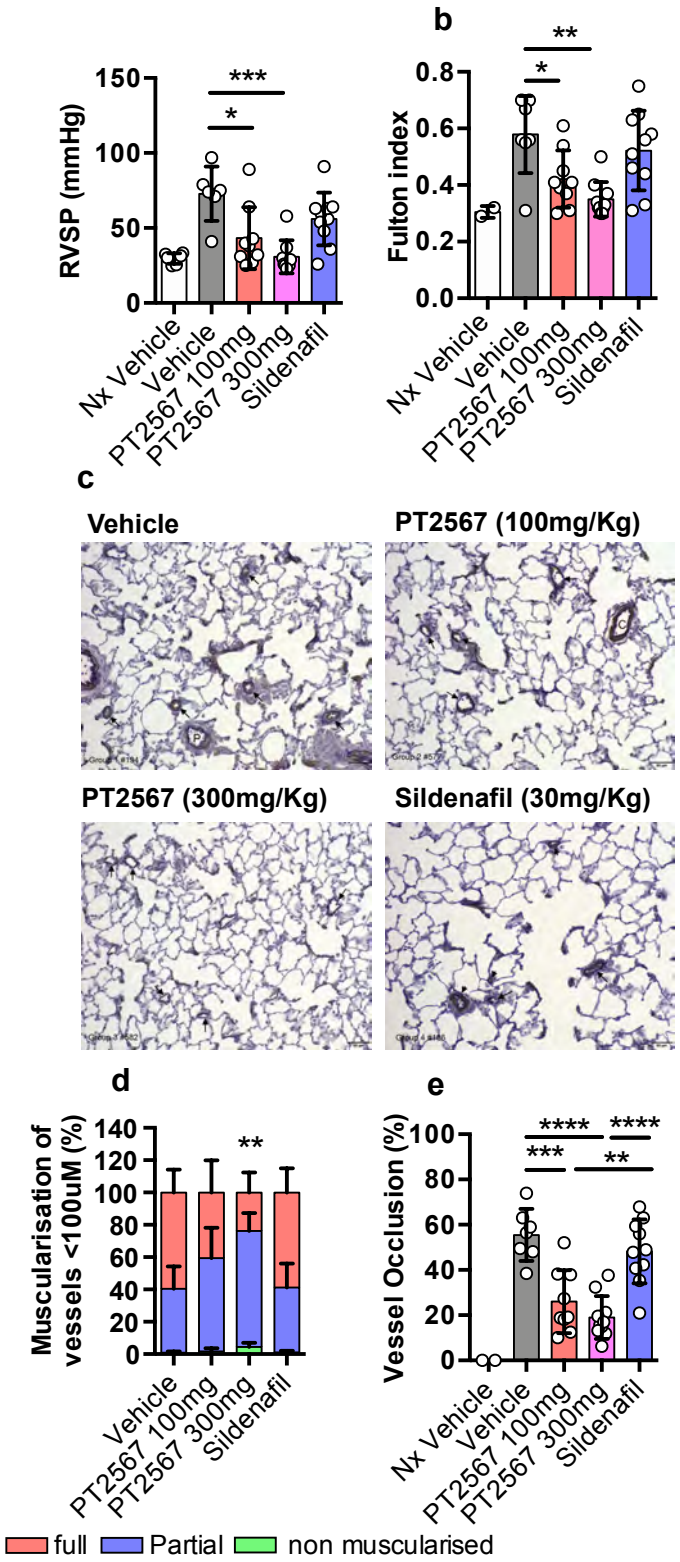

Figure 1. Effect of HIF2α-inhibitor on the development of PAH in a rat SU-5416/Hx prevention model.
a, b (a) RVSP. (b) RVH showing RV/LV+S weight ratio in Sprague-Dawley (SD) Su5416/Hx rats gavaged q.d. with vehicle (n=7), PT2567 100mg/kg (n=9) or 300mg/kg (n=9), or 30mg/kg Sildenafil (n=10).
c Representative photomicrographs immune-stained for α-SMA (arrows point to distal vessels, scale-bar 50μM)
d Stacked-bar chart showing quantification of muscularisation of peripheral pulmonary vessels in lung sections (green bar, no smooth muscle ring; blue bar, partial smooth muscle ring; red bar full smooth muscle ring)
e Determination of small arterial vessel (>50μM) occlusion, shown as percentage fully occluded
Data information mean ± SD *p<0.05, **p<0.001, ***p<0.0001 ****p<0.00001 (one-way ANOVA)

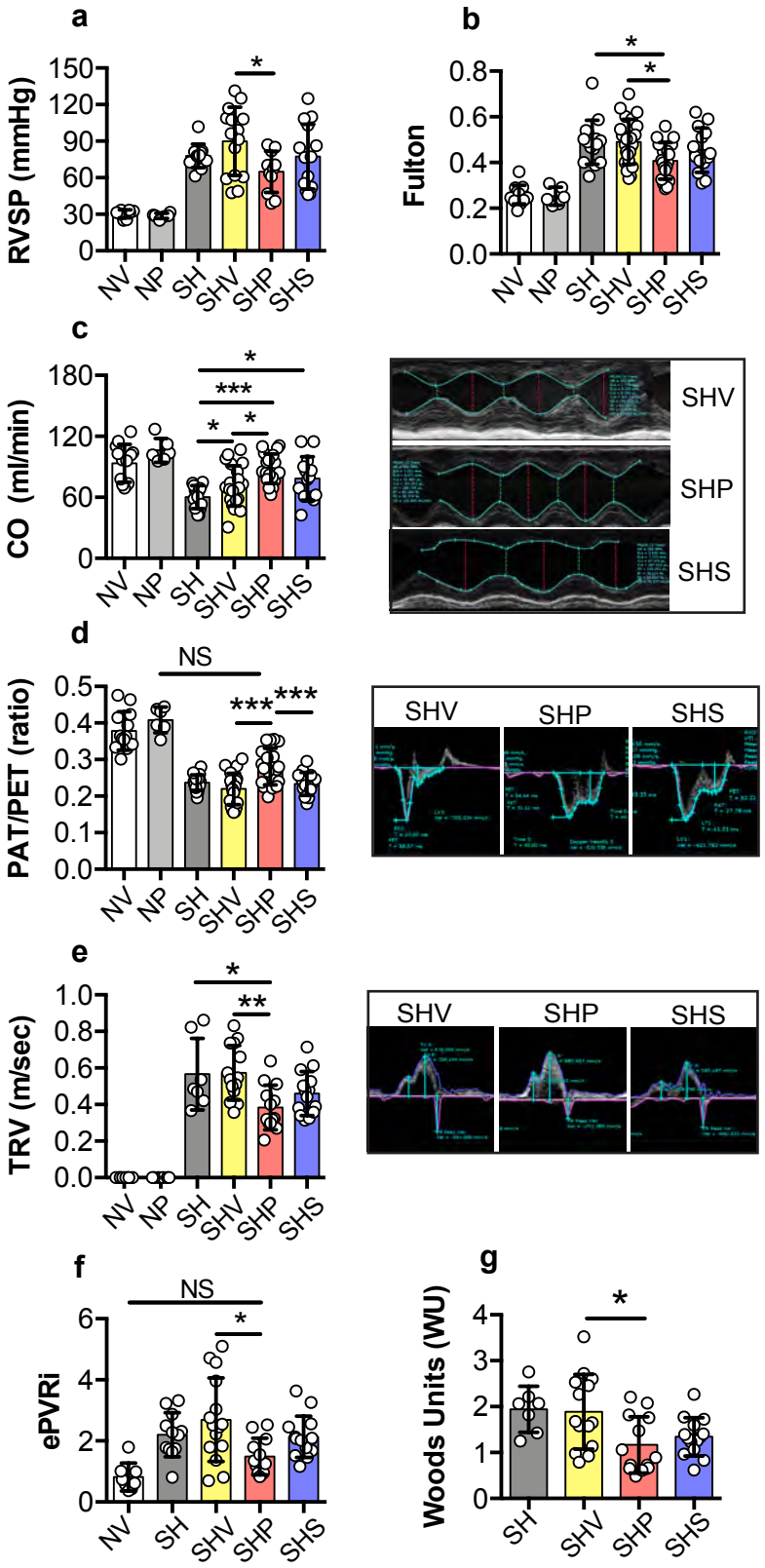

(Normoxia/Vehicle=**NV**, Normoxia/PT2567=**NP,** Su/Hx-3w=**SH**, Su/Hx/Veh=**SHV**, Su/Hx-PT2567=**SHP**, Su/Hx-Sildenafil=**SHS**)

Figure 2. HIF2α-inhibitor decreases pulmonary vascular resistance in established rat Su5416/Hx PH model.

a-c (a) assessment of RVSP and (b) RVH, (c) cardiac output in Sprague-Dawley rats

d, e Cardiac echo analysis of (d) PAT/PET ratio with representative photomicrographs (e) TVR-velocity with representative photomicrographs for vehicle control, PT2567 or sildenafil.

f, g Calculation of pulmonary vascular resistance (f) Estimation-PVR index. (g) Woods units.

Data information, mean ± SD, Nx/Veh (n=8) Su/Hx-3w (n=12) Su/Hx-Vehicle (n=15) Su/Hx-PT2567 (n=15) Su/Hx-sildenafil (n=14) *p<0.05, **p<0.001, ***p<0.0001 (one-way ANOVA)

Figure 3

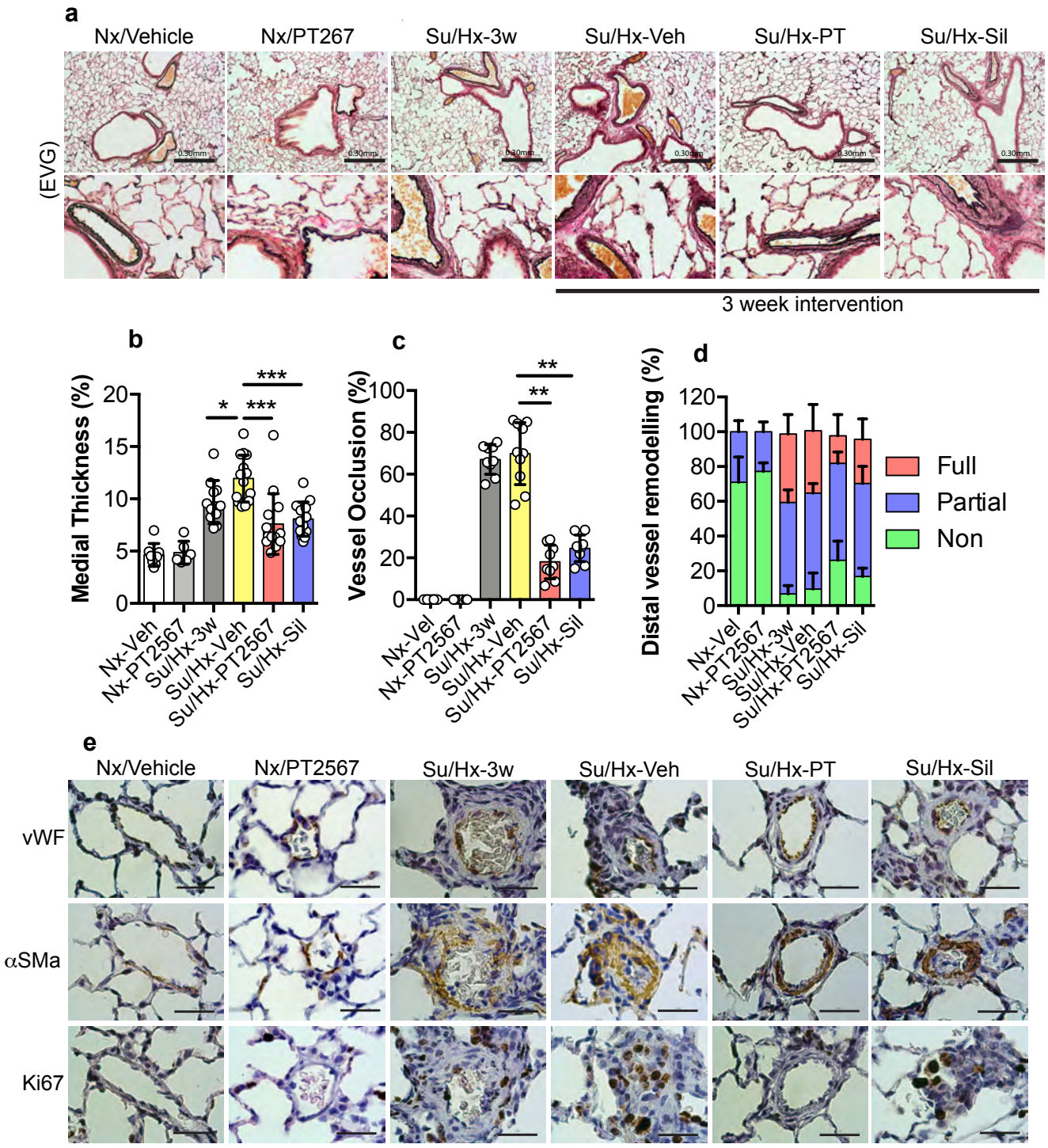

Figure 3. **PT2567 decreases pulmonary vascular remodelling**

a Representative photomicrographs of lung sections stained with elastic van Gieson (EVG) (scale bar 0.30mm)

b Assessment of PA wall thickness as a percentage of luminal diameter

c Determination of small arterial vessel (>50μM) occlusion, shown as percentage fully occluded.

d Quantification of non-, partially- and fully-muscularised arteries as a percentage of total alveolar wall and duct arteries.

e Representative photomicrographs of lung sections imuno-stained for von-Willibrand Factor, α-SMA and Ki67 (scale bar 0.30mm) Data information mean ± SD (Nx/Veh n=8, Nx/PT2567 n=6, SuHx-3w n=12, SuHx Veh n=15, SuHx-PT2567 n=11, SuHx-sildenafil n=14). *p<0.05, **p<0.001, ***p<0.0001 (one-way ANOVA)

Figure 4

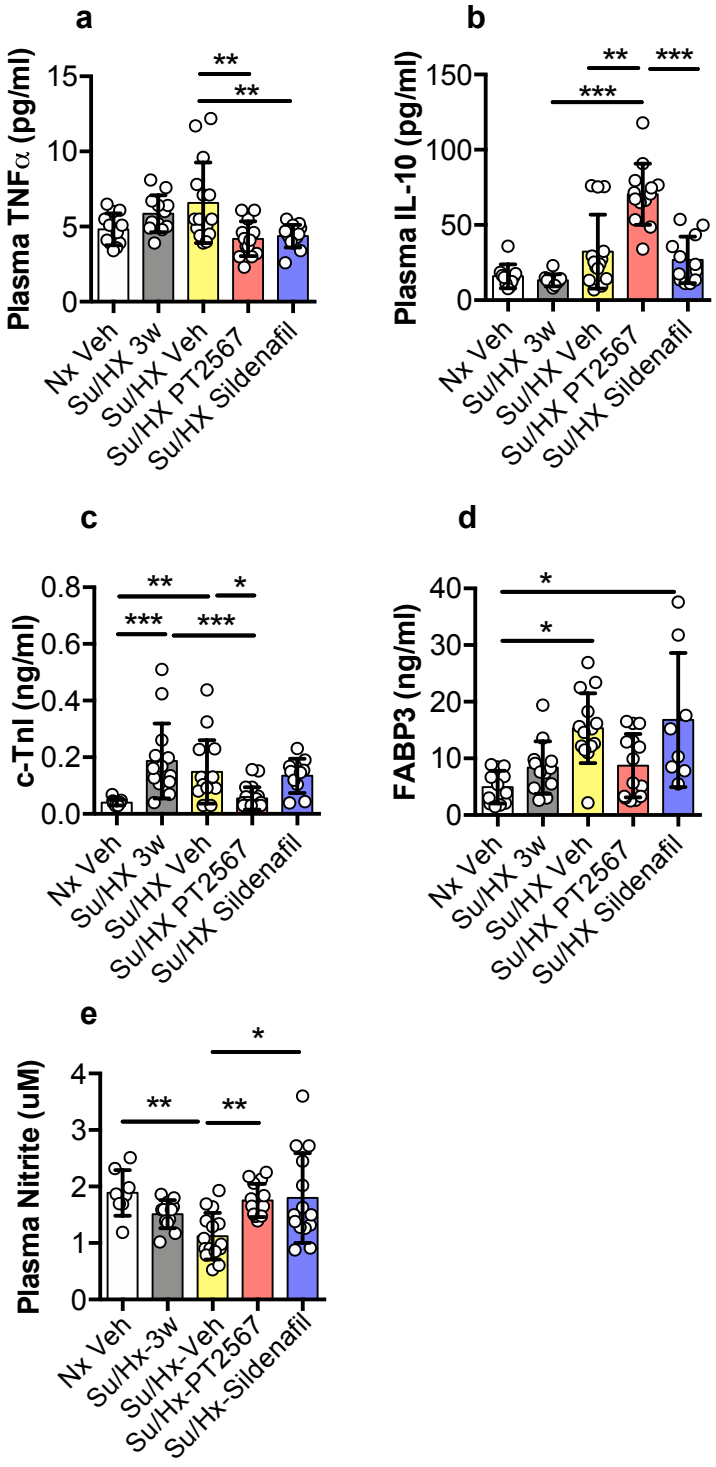

Figure 4. **HIF2α-inhibition restores plasma nitrite levels.**
a-d Plasma cytokines and cardiac stress factor analysis (a) TNFα, (b) IL-10, (Nx/Veh n=8, SuHx n=12, SuHx Veh n=15, SuHx PT2567 n=11, SuHx sildenafil n=14). (c) c-TnI (d) FABP3, (Nx/Veh n=6, Su/Hx-3w n=6, Su/Hx-Veh n=8, Su/Hx-PT2567 n=8, Su/Hx-sildenafil n=8).
e Plasma nitrite assessed by NO analyser (Sievers) (Nx/Veh n=8, Su/Hx-3w n=12, Su/Hx-Veh n=15, Su/Hx-PT2567 n=11, SuHx-sildenafil n=14).
Data information, mean ± SD *p<0.05, **p<0.001, ***p<0.0001 (one-way ANOVA)

Figure 5

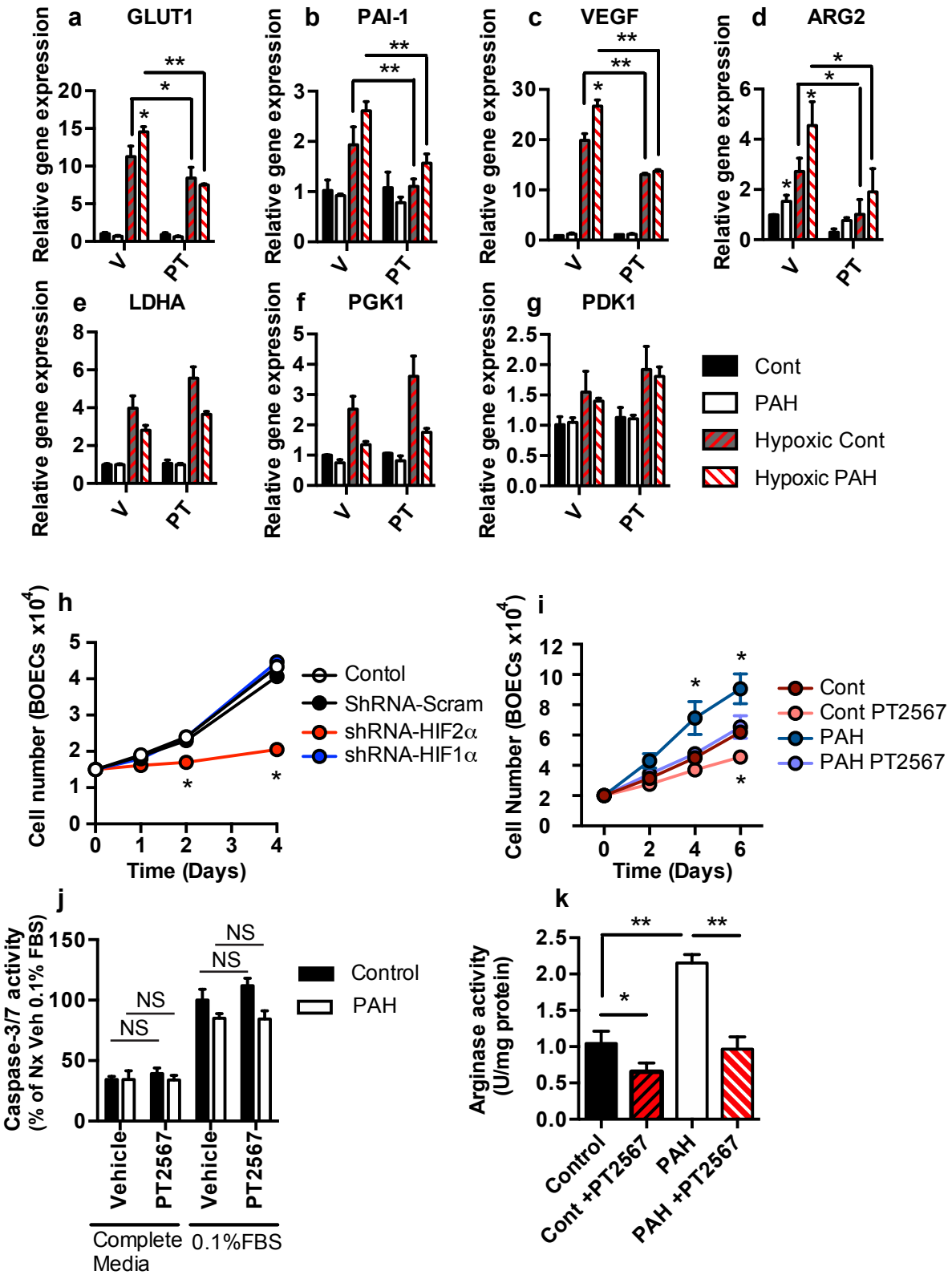

Figure 5. **Analysis of human BOECs as a model for studying in vitro endothelial function in PAH.**
a-g Human BOECs were exposed to hypoxia +/- PT2567 (PT) or vehicle (V), gene expression determined by qPCR (a) GLUT1, (b) PAI-1 (c) VEGF (d) Arg2 (e) LDHA (f) PGK1 (g) PDK1.
h Control BOEC proliferation following HIFα knock-down.
i Control and PAH BOEC proliferation +/- PT2567
j BOEC apoptosis determined by caspase-3/7 activity. BOECs were culture in complete endothelial media or basal endothelial media with 0.1%-FBS +/- PT2567 for 18 hr. Data corrected to positive control (0.1% FBS control BOECs with vehicle) percentage mean activity ± SEM.
k Arginase activity assay from control and PAH BOEC +/- PT2567
Data information hBOECs from healthy volunteers (n=3) or PAH patients (n=3) mean ± SEM.
*p<0.05, **p<0.001 (one-way ANOVA)

Supplemental tables 1a Prevention-protocol pulmonary histology assessment

Group	Animal	Perivascular/vascular inflammation	Perivascular fibrosis	Smooth muscle hypertrophy
1 Vehicle	1	0	0	2
	2	2	1	4
	3	1	1	4
	4	0	0	4
	5	1	1	4
	6	2	1	4
	7	1	1	4
	Mean score	**5.42**		

Group	Animal	Perivascular/vascular inflammation	Perivascular fibrosis	Smooth muscle hypertrophy
2 PT2567 100mg /kg	1	0	0	2
	2	1	0	3
	3	1	0	3
	4	0	0	2
	5	0	0	3
	6	1	1	4
	7	0	0	3
	8	1	1	4
	9	0	0	3
	Mean Score	**3.66**		

Group	Animal	Perivascular/vascular inflammation	Perivascular fibrosis	Smooth muscle hypertrophy
3 PT2567 300mg /kg	1	0	0	2
	2	0	1	4
	3	1	1	3
	4	0	0	2
	5	0	0	2
	6	0	0	2
	7	0	0	2
	8	0	0	2
	9	0	0	1
	Mean Score	**2.55**		

Group	Animal	Perivascular/vascular inflammation	Perivascular fibrosis	Smooth muscle hypertrophy
4 Sildenafil 30mg /kg	1	0	0	2
	2	0	0	3
	3	1	0	4
	4	0	0	3
	5	0	0	4
	6	1	1	4
	7	2	0	4
	8	0	1	3
	9	1	0	4
	10	0	0	3
	Mean Score	**4.00**		
5 Nx Control	1	0	0	0
	2	0	0	0
	Mean Score	**0**		

The number represents the grade (0=normal, 1=minimal, 2=mild, 3=moderate, 4=marked) for each lesion/finding

Supplemental tables 1b Intervention-protocol pulmonary histology assessment

Group	Animal	Perivascular/vascular inflammation	Perivascular fibrosis	Smooth muscle hypertrophy
1 Nx-Vehicle	1	0	0	0
	2	0	0	0
	3	0	0	1
	4	1	0	1
	5	0	1	0
	6	0	0	0
	Mean score	**0.66**		

Group	Animal	Perivascular/vascular inflammation	Perivascular fibrosis	Smooth muscle hypertrophy
2 Su/Hx 3W	1	3	2	2
	2	2	1	2
	3	2	2	3
	4	2	1	2
	5	2	1	2
	6	3	2	3
	7	2	2	2
	8	2	2	2
	9	3	3	3
	10	3	2	3
	Mean Score	**5.7**		

Group	Animal	Perivascular/vascular inflammation	Perivascular fibrosis	Smooth muscle hypertrophy
3 Su/Hx Vehicle	1	3	3	4
	2	3	3	2
	3	4	3	4
	4	2	2	3
	5	4	3	2
	6	2	2	2
	7	4	3	4
	8	2	3	4
	9	2	2	3
	10	3	3	4
	Mean Score	**8.9**		

Group	Animal	Perivascular/vascular inflammation	Perivascular fibrosis	Smooth muscle hypertrophy
4 Su/Hx PT2567 100mg/kg	1	2	1	1
	2	1	1	1
	3	1	1	1
	4	2	2	1
	5	1	1	2
	6	0	1	1
	7	1	1	1
	8	2	1	2
	9	3	2	3
	10	3	3	4
	Mean Score	**4.7**		

Group	Animal	Perivascular/vascular inflammation	Perivascular fibrosis	Smooth muscle hypertrophy
5 Su/H Sildenafil	1	2	2	2
	2	2	1	1
	3	4	2	3
	4	3	2	2

30mg/kg	5	2	2	3
	6	2	2	2
	7	2	2	2
	8	2	1	1
	9	1	1	2
	10	3	2	2
	Mean Score	**5.9**		

The number represents the grade (0=normal, 1=minimal, 2=mild, 3=moderate, 4=marked) for each lesion/finding

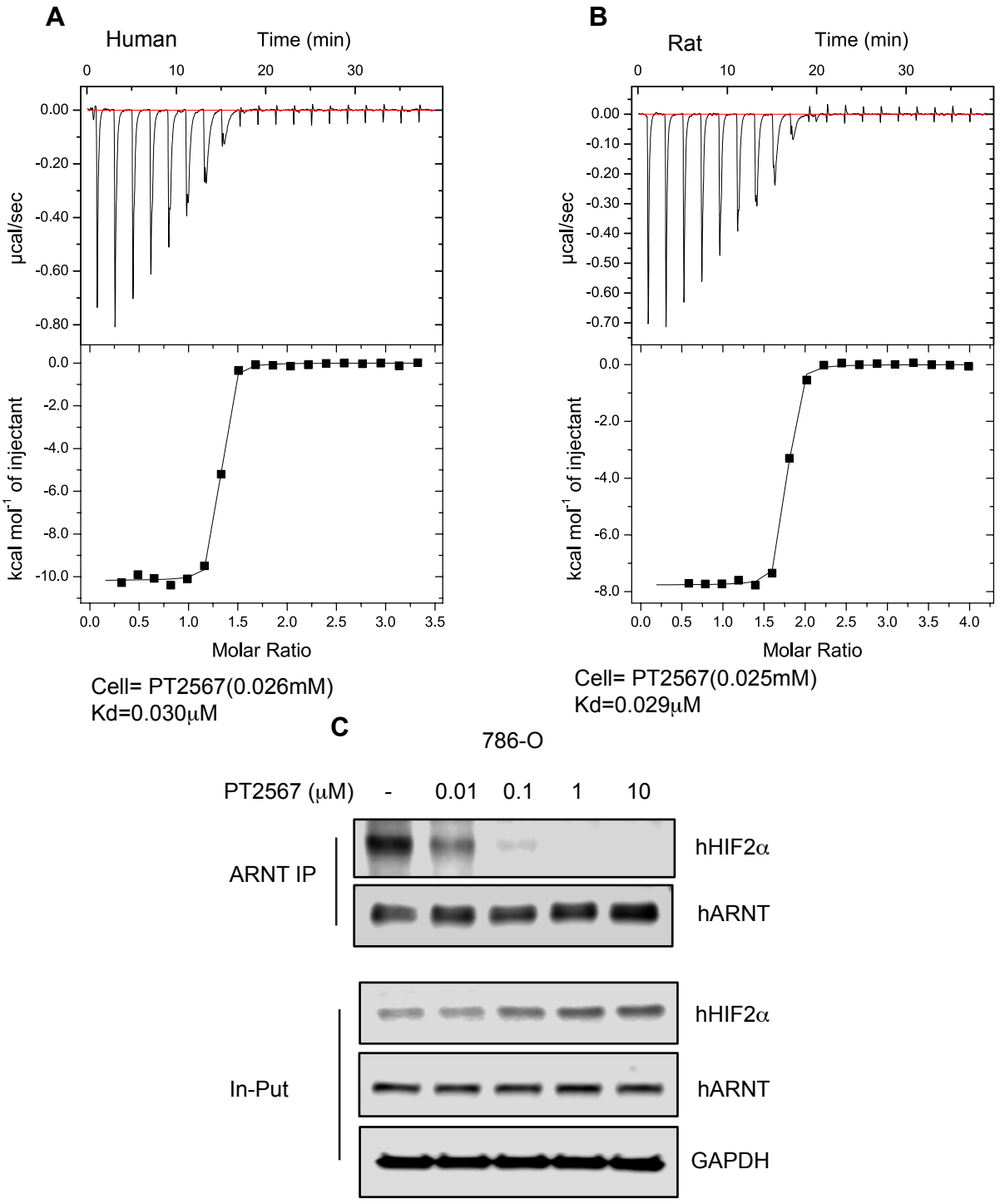

Figure S1. Binding of PT2567 to HIF2α PAS-B domain disrupts HIF2α/ARNT dimer formation.
A, B Binding affinity of PT2567 to PAS-B domain of (A) human HIF2α and (B) rat HIF2α using isothermal titration calorimetry.
C Co-immunoprecipitation experiment in 786-O cells demonstrating PT2567 disrupts HIF2α/ARNT dimerization

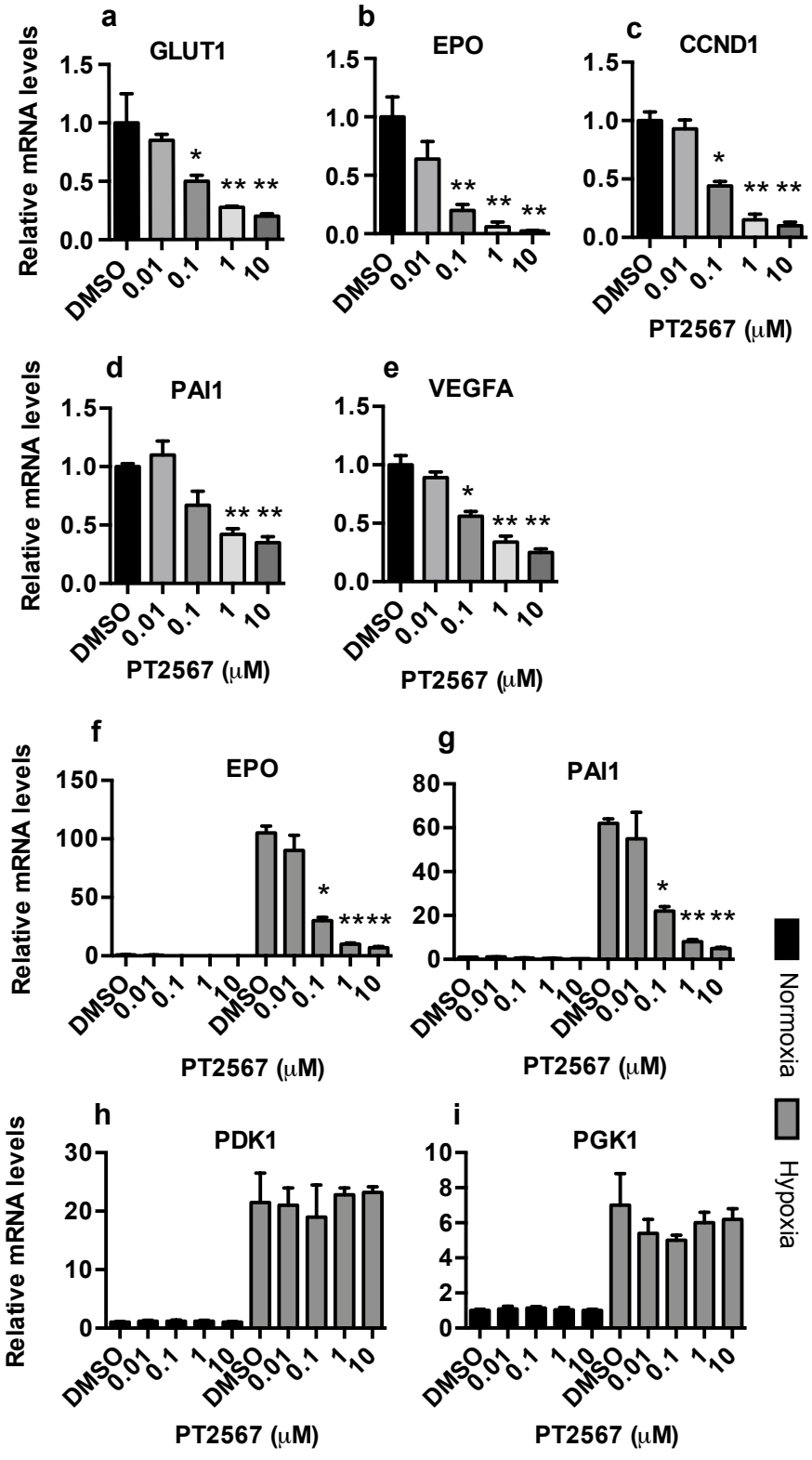

Figure S2. **PT2567 selectively inhibits HIF2α-target gene expression in 786-O and Hep3B cells.**
a-e PT2567 reduces 786-O mRNA levels for (a) GLUT1 (b) EPO, (c) CCDN1, (d) PAI1, and (e) VEGFA.
f-i PT2567 inhibits hypoxic stimulated HIF2α target gene expression (f) EPO, and (g) PAI1 without influencing HIF1α target genes (h) PDK1 and (i) PGK1 in Hep3B cells.
Data information mean ± SD (n=5) *p<0.05, **p<0.001 (one-way ANOVA)

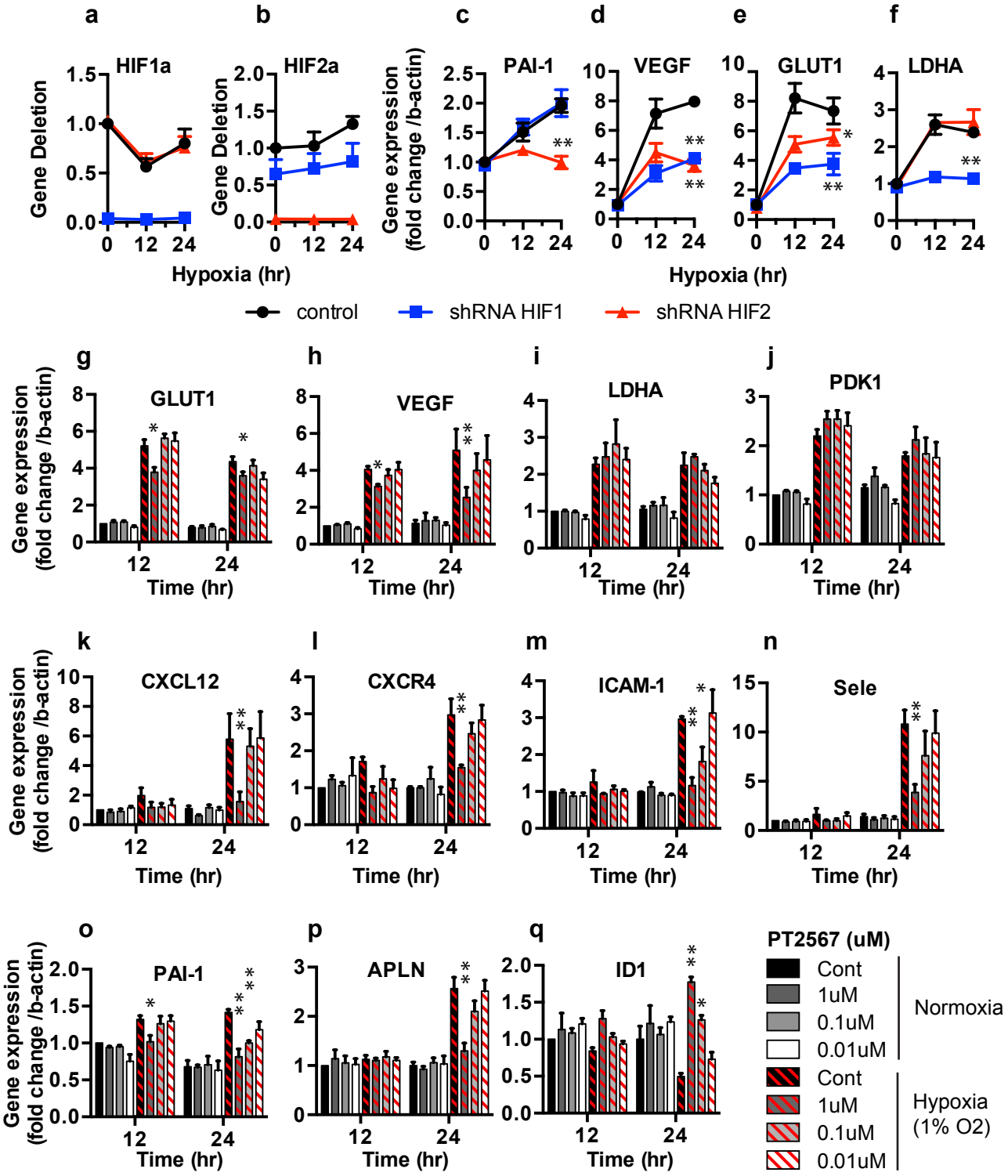

Figure S3. **Validation of PT2567 specificity and activity in hPAEC.**
a-f Human-PAECs were exposed to hypoxic time course +/- sh-RNA-HIF1α or –HIF2α, gene expression determined by qPCR (a) HIF1α, (b) HIF2α, (c) PAI-1, (d) VEGF, (e) GLUT1, (f) LDHA.
g-k PT2567 concentration response in hypoxia exposed hPAEC, gene expression determined by qPCR (g) GLUT1 (h) VEGF, (i) LDHA, (j) PDK1, (k) CXCL12, (l) CXCR4 (m) ICAM-1, (n) Sele, (o) PAI-1, (p) APLN, (q) ID1
Data information mean ± SEM (n=3) *p<0.05, **p<0.001 (T-Test)

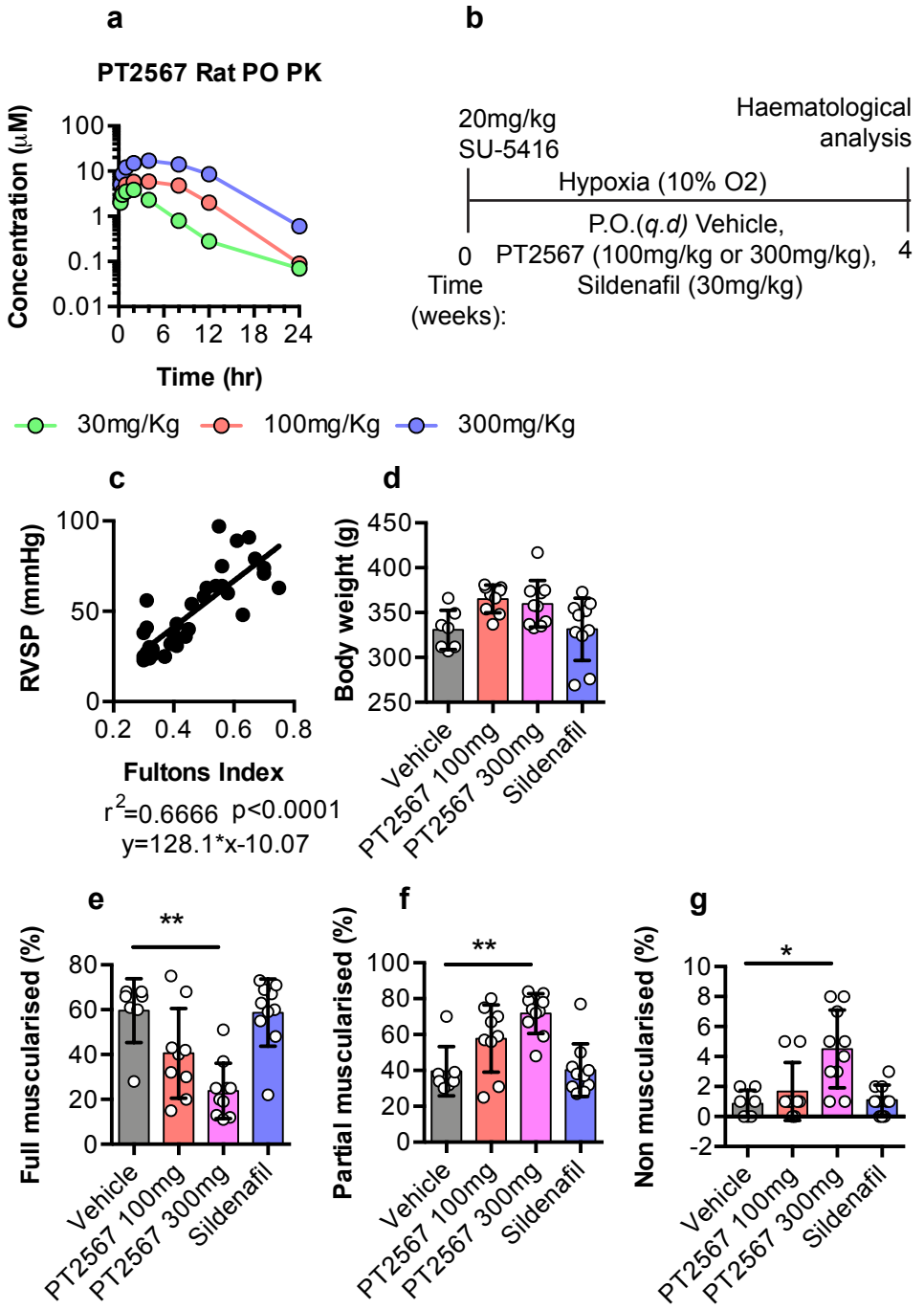

Figure S4. **Rat PT2567 PO PK and PAH prevention profiles**
a Plasma concentration versus time profiles of PT2567 after oral administration of 30, 100, 300mg/Kg.
b Line-diagram depicting the rat PH treatment strategy.
c Assessment of correlation between RVSP and RVH in the SU-5416 hypoxia prevention model (r2=0.666, y=128.1*x-10.07).
d Final body weight (g)
e-g Quantification of distal muscularisation process characterised as (e) fully muscularised, (f) partially muscularised or (g) non-muscularised.
Data Information mean ± SD (SuHx Veh n=8, SuHx PT2567 (100mg/kg) n=9 (300mg/kg) n=10, SuHx sildenafil n=10)*p<0.05, **p<0.001 (one-way ANOVA)

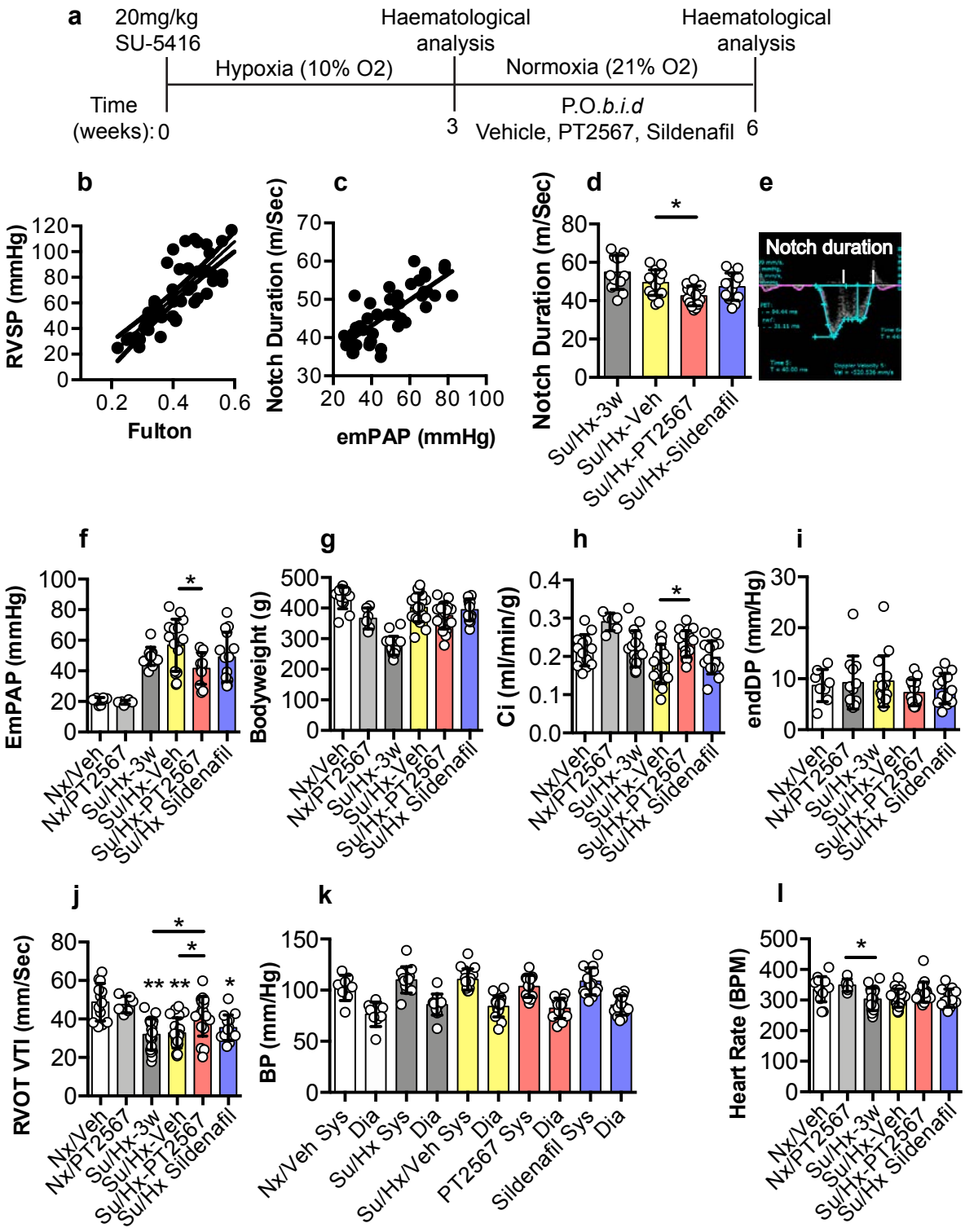

Figure S5 PT2567 restores PAT in a SU-5416/Hx intervention model of PH.
a Line-diagram depicting the rat PH treatment strategy
b, c Assessment of correlation between (b) RVSP and RVH in the SU-5416/Hx intervention model (r2=0.7066, y=0.220.3x-24.25, p<0.0001). (c) Notch duration and emPAP in the SU-5416/Hx intervention model (r2=0.5944, y=0.3381*x29.58).
d, e Cardiac echo was used to determine (d) Notch duration (e) Representative image showing Notch duration.
f-j Parameters used to calculate PVR (f) Estimation-PAP (mm/Hg) (g) Final body weight (g) (h) Cardiac-index (mmHg/g) (i) End diastolic pressure (mmHg) (j) RVOT VTI.
k Assessment of left ventricle function (mm/Hg) h, heart rate following intervention with vehicle, PT2567 or sildenafil, Data information mean ± SD Nx/Veh n=8-11, Nx/PT2567 n=6, SuHx-3w n=12-18, SuHx-Veh n=15-22, SuHx-PT2567 n=11-19, SuHx-sildenafil n=14. *p<0.05, **p<0.001 (one-way ANOVA)

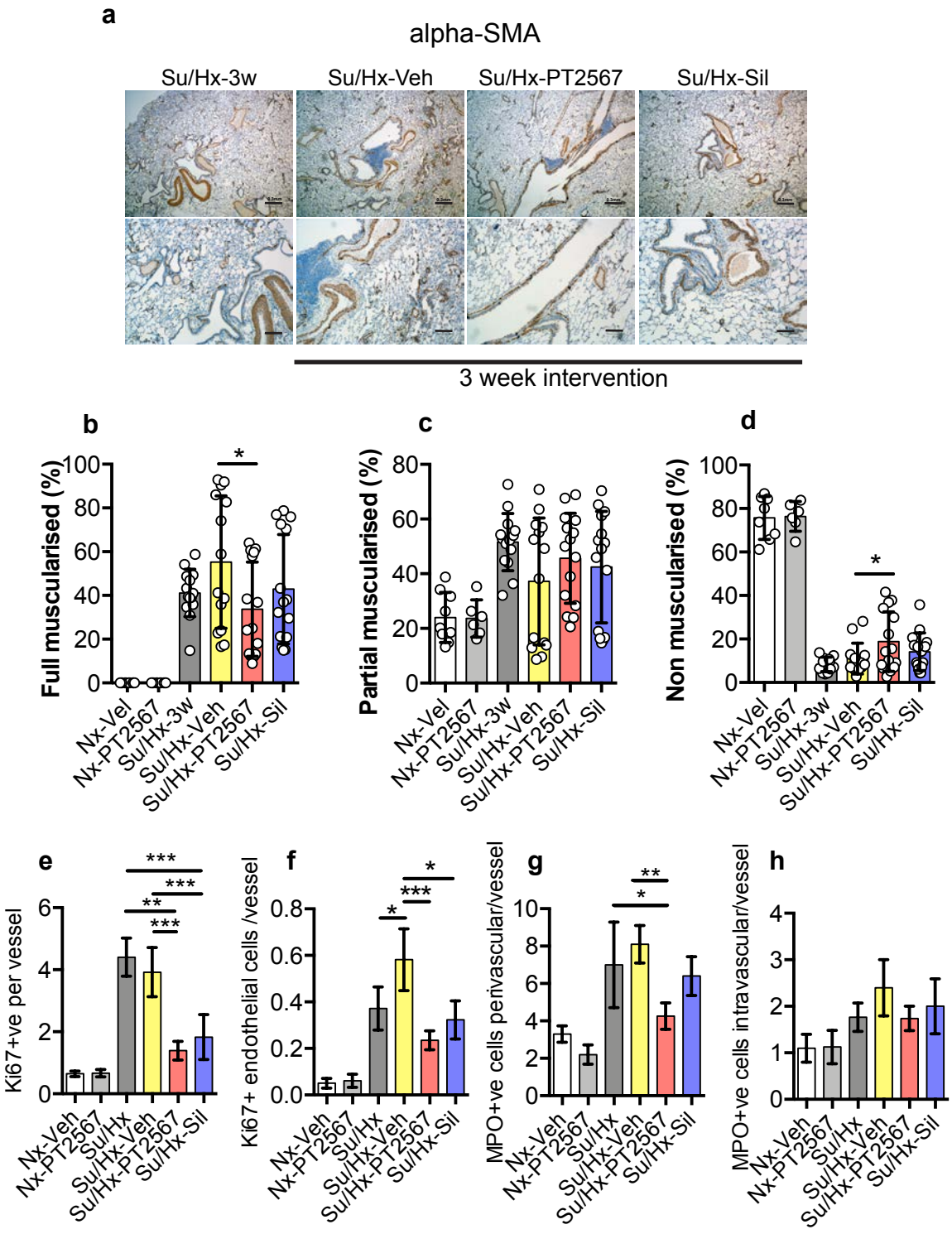

Figure S6 PT2567 intervention reduces pulmonary vascular remodeling
a Representative photomicrographs showing histological analysis of αSMA in lung sections. Scale bar on 0.3mm.
b-d Quantification of lung histological sections stained with αSMA. Distal muscularisation process characterised as (b) fully muscularised, (c) partially muscularised or (d) non-muscularised. Data information mean ± SD Nx/Veh n=8, SuHx-3w n=12, SuHx-Veh n=15, SuHx-PT2567 n=11, SuHx-sildenafil n=14.
e-f Bar chart of the number of (e) Ki67+ nuclei per vessel, (f) Ki67+ endothelial cells per vessel
g-h Bar chart of MPO immuno-positive cells perivascular (**g**) and intravascular (**h**) Data information mean ± SD Nx/Veh n=3, Nx/PT2567 n=3, SuHx-3w n=3, SuHx-Veh n=4, SuHx-PT2567 n=5, SuHx-sildenafil n=4. *p<0.05 **p<0.01 ***p<0.001 (one-way ANOVA)

Lung gene expression

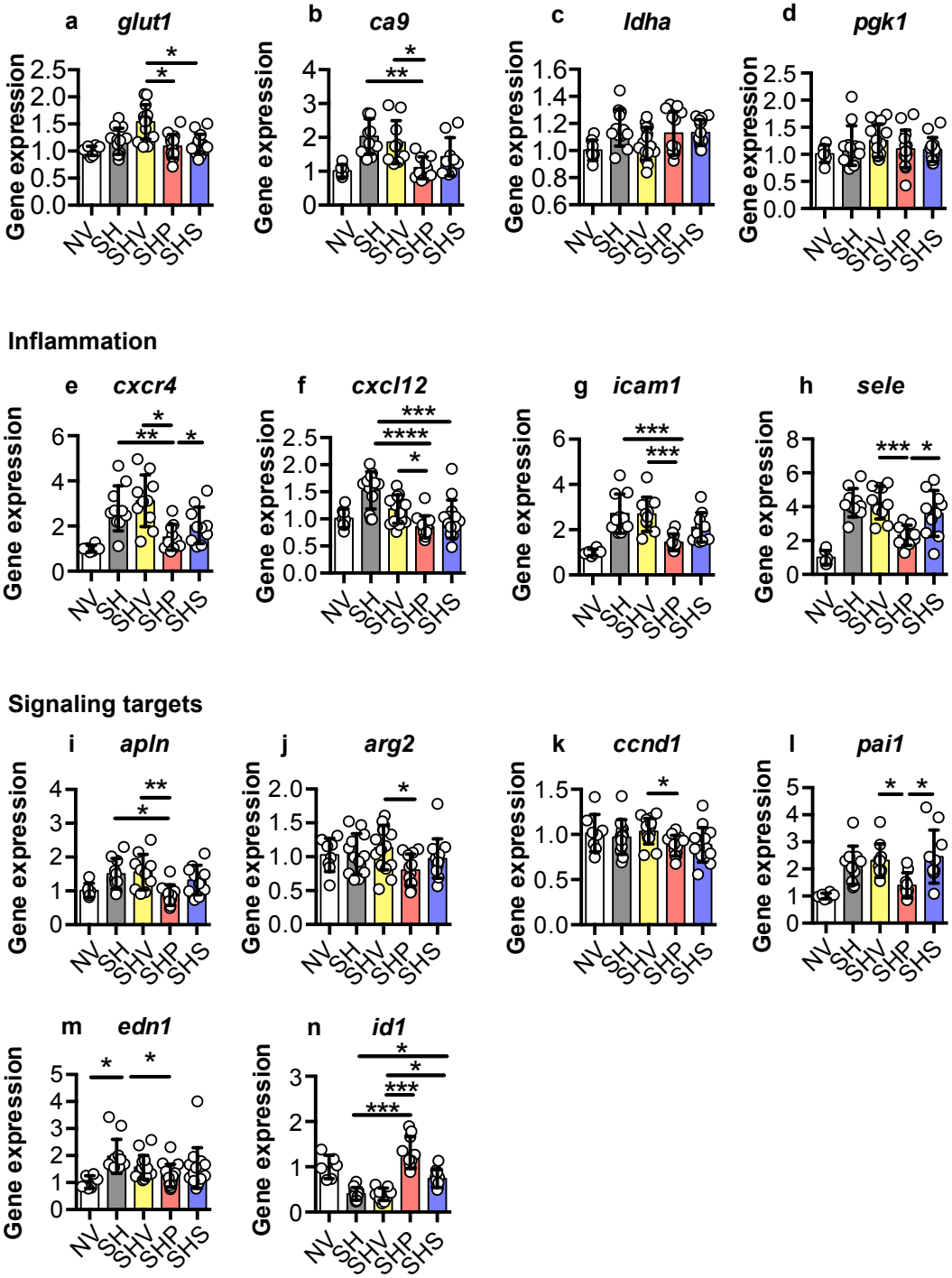

Figure S7 Inhibition of HIF2a with PT2567 modulates the expression of lung gene from Su/Hx rats
a-n qPCR analysis of whole lung samples (a) glut1, (b) ca9 (c) ldha, (d) pgk1, (e) cxcr4, (f) cxcl12, (g) icam1, (h) sele, (i) apln, (j) arg2, (k) ccnd1, (l) pai1, (m) edn1, (n) id1.
Data information mean ± SD rat Su5416/Hx intervention model (Nx/Veh n=8, Su/Hx-3w n=12, Su/Hx-Veh n=15, Su/Hx-PT2567 n=11, Su/Hx-sildenafil n=14). Data show fold change in gene expression relative to Nx/Veh control rats.*p<0.05, **p<0.001, ***p<0.001, ****p<0.0001(one-way ANOVA)
NV normoxia-vehicle, SH Sugen hypoxia 3 weeks, SHV Sugen hypoxia vehicle, SHP Sugen hypoxia PT2567 SHS Sugen hypoxia sildenafil

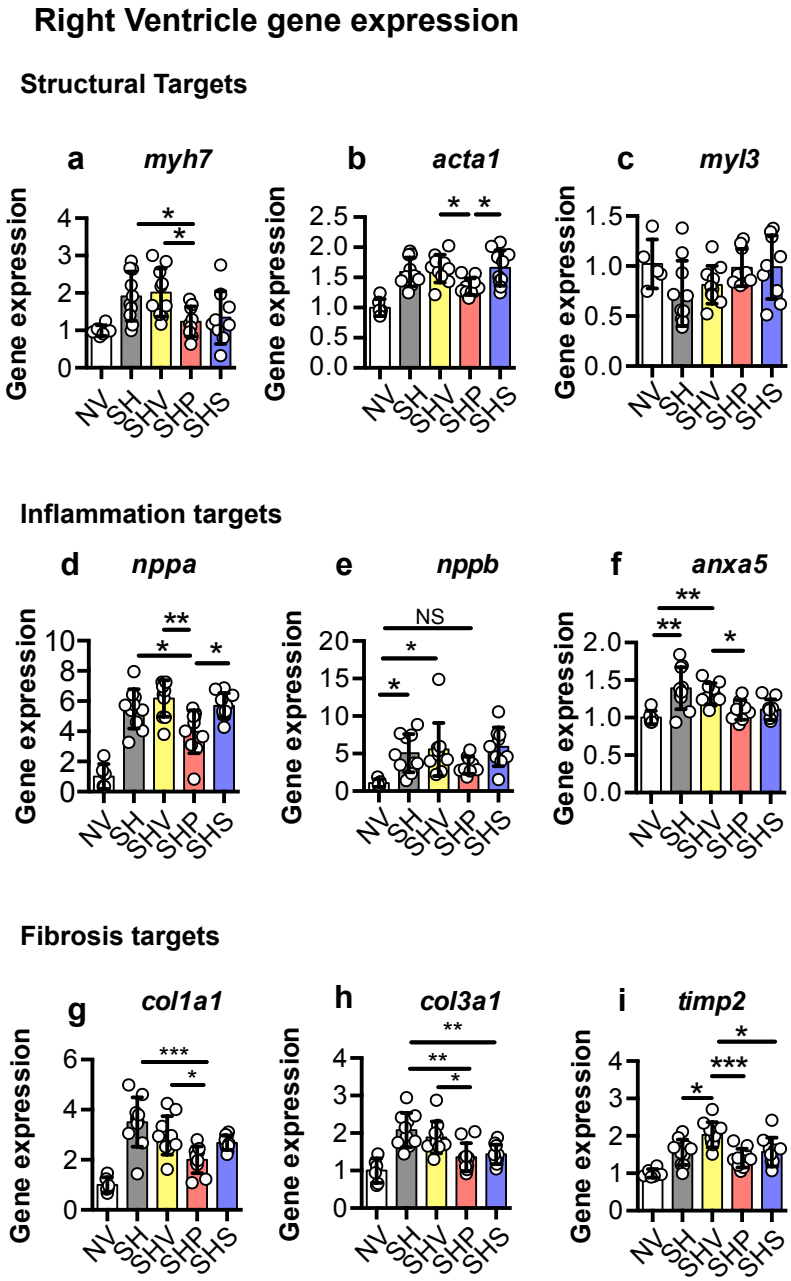

Figure S8 PT2567 modulates cardiac target gene expression in Su/Hx rats
a-i qPCR analysis of RV samples (a) myh7, (b) myl3, (c) acta1, (d) nppa, (e) nppb, (f) anxa5, (g) col1a1, (h) col3a1, (i) timp2.
Data information mean ± SD rat Su/Hx intervention model (Nx/Veh n=8, Su/Hx-3w n=12, Su/Hx-Veh n=15, Su/Hx-PT2567 n=11, Su/Hx-sildenafil n=14). Data show fold change in gene expression relative to Nx/Veh control rats.*p<0.05, **p<0.001, ***p<0.0001 (one-way ANOVA)
NV normoxia-vehicle, SH Sugen hypoxia 3 weeks, SHV Sugen hypoxia vehicle, SHP Sugen hypoxia PT2567 SHS Sugen hypoxia sildenafil

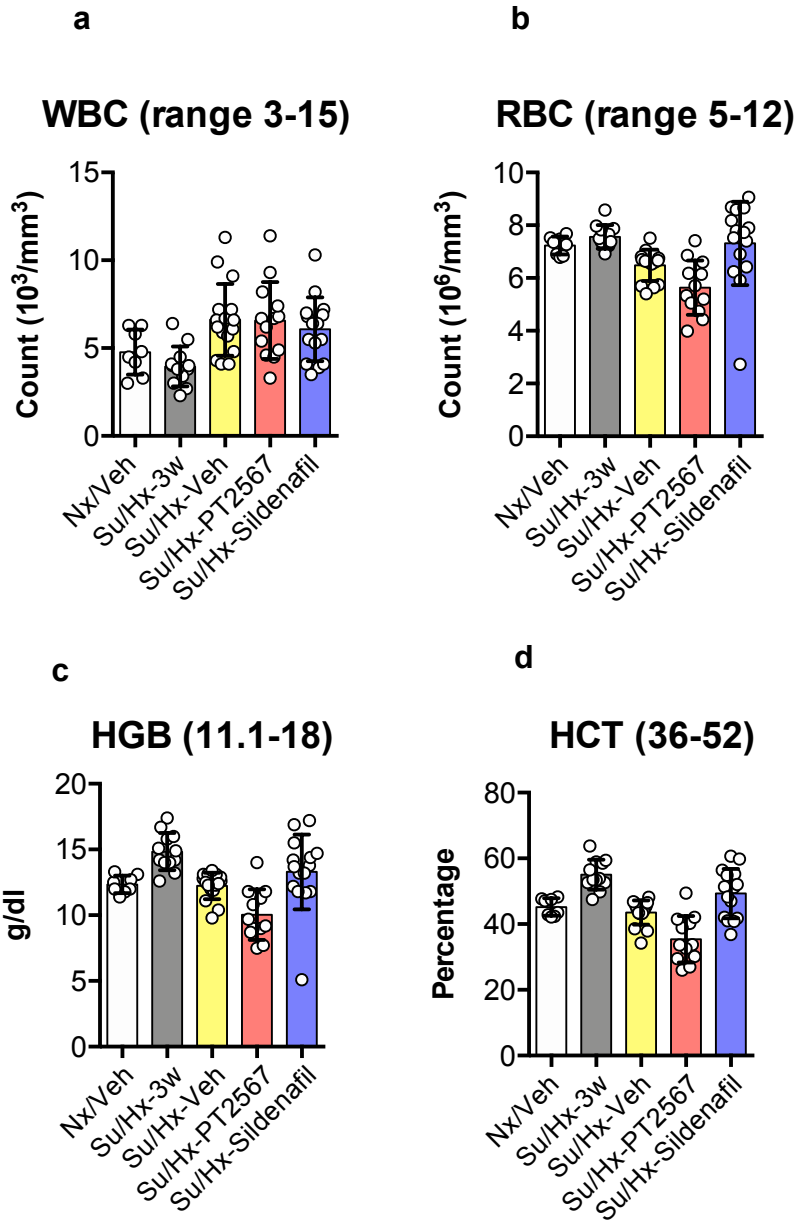

Figure S9. **HIF2α inhibitor decreases RBC, HGB and HCT to lower physiological counts.**
a-d Whole blood analysis (a) WBC, (b) RBC, (c) HGB and (d) HCT
Data information mean ± SD (Nx/Veh n=8, Su/Hx-3w n=12, Su/Hx-Veh n=15, Su/Hx-PT2567 n=11, Su/Hx-sildenafil n=14).

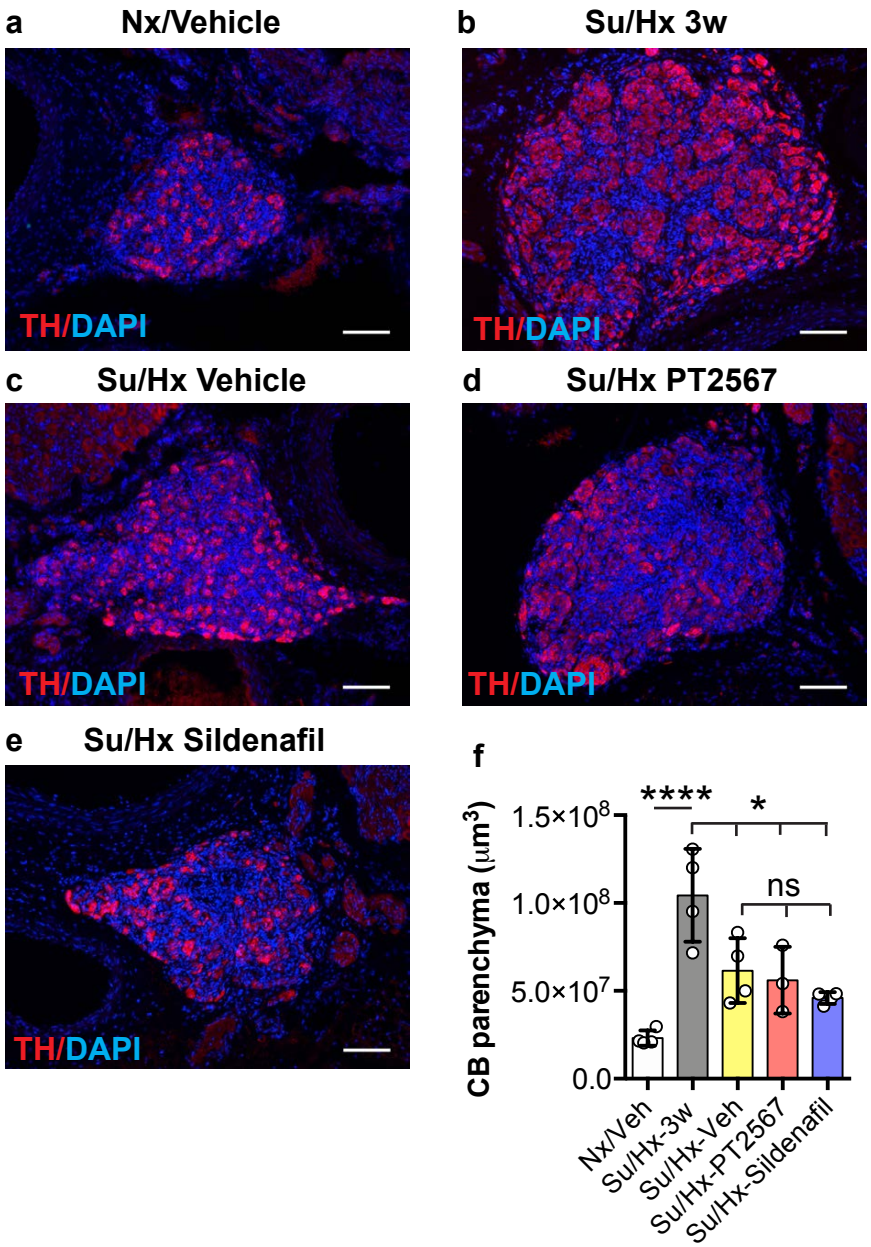

Figure S10. **PT2567 does not alter carotid body morphology.**
a-e Tyrosine hydroxylase (TH) immunostaining of the carotid bifurcation from rats exposed to the indicated treatments. Scale bars: 100 μm.
f CB volume quantification across the treatments.
Data information mean ±SEM Nx/Veh n=4, SuHx 3W n=4, SuHx Veh n=4, SuHx PT2567 n=3, SuHx sildenafil n=4. ****p<0.0001, *p<0.05, ns = non-significant (T-Test).

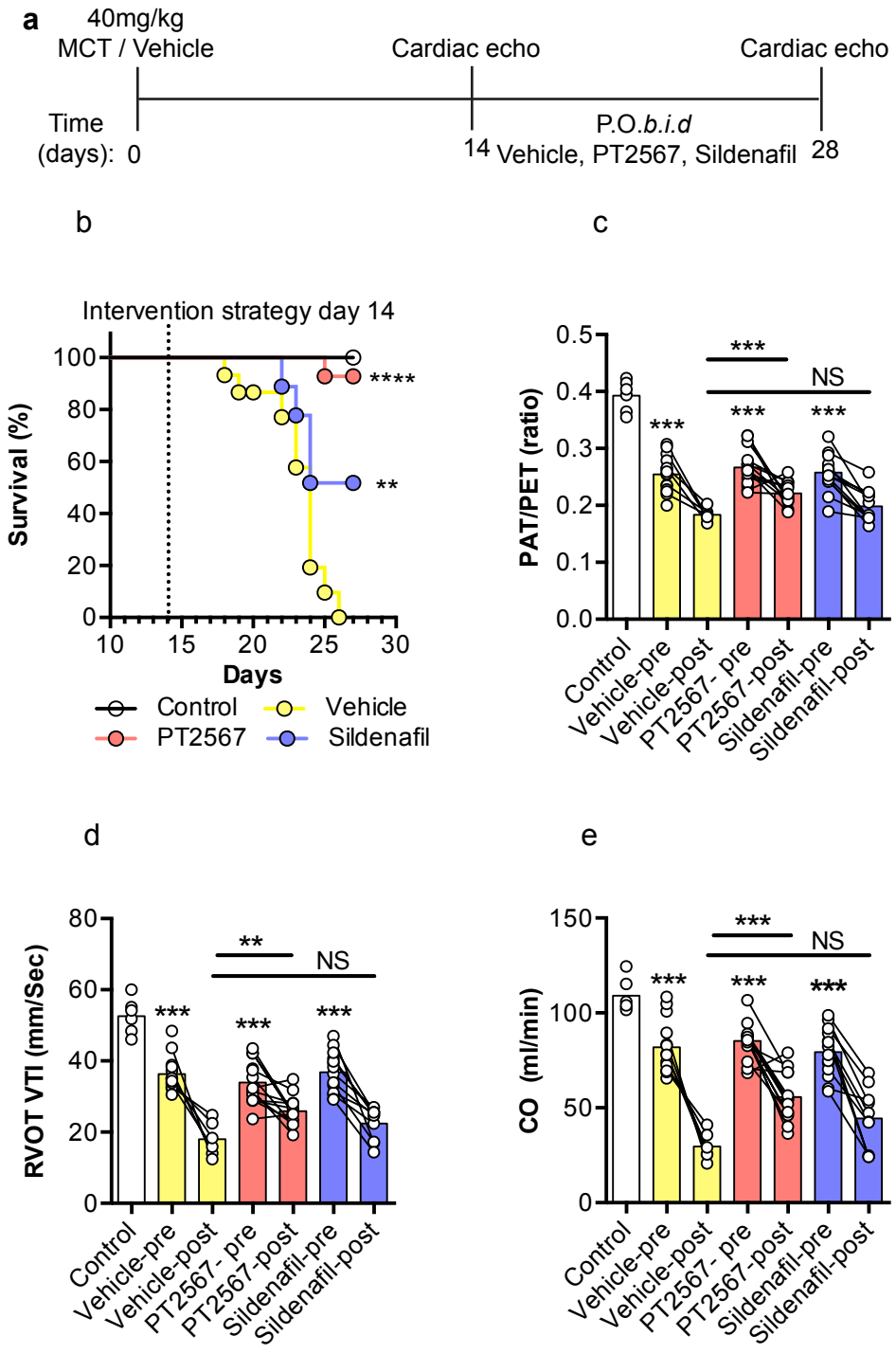

Figure S11. PT2567 treatment promotes survival in monocrotaline PH model.
(a) Line diagram showing the experimental time line of monocrotaline (MCT) rat PH model, (b) PT2567 intervention inceased the survival rate of MCT treated animals when compared to sildenafil and vehicle controls. (c-e) Cardiac echo analyses pre- and post-intervention identified that PT2567 treatment reduced cardiac dysfunction, (c) PAT/PET ratio, (d) RVOT-VTI (e) cardiac output (CO) Kaplan-meier survival analysis assessed by log-rank (Mantel-Cox) test Data information, mean **p<0.001, ***p<0.0001 ****p<0.00001(one-way ANOVA)

Figure S12

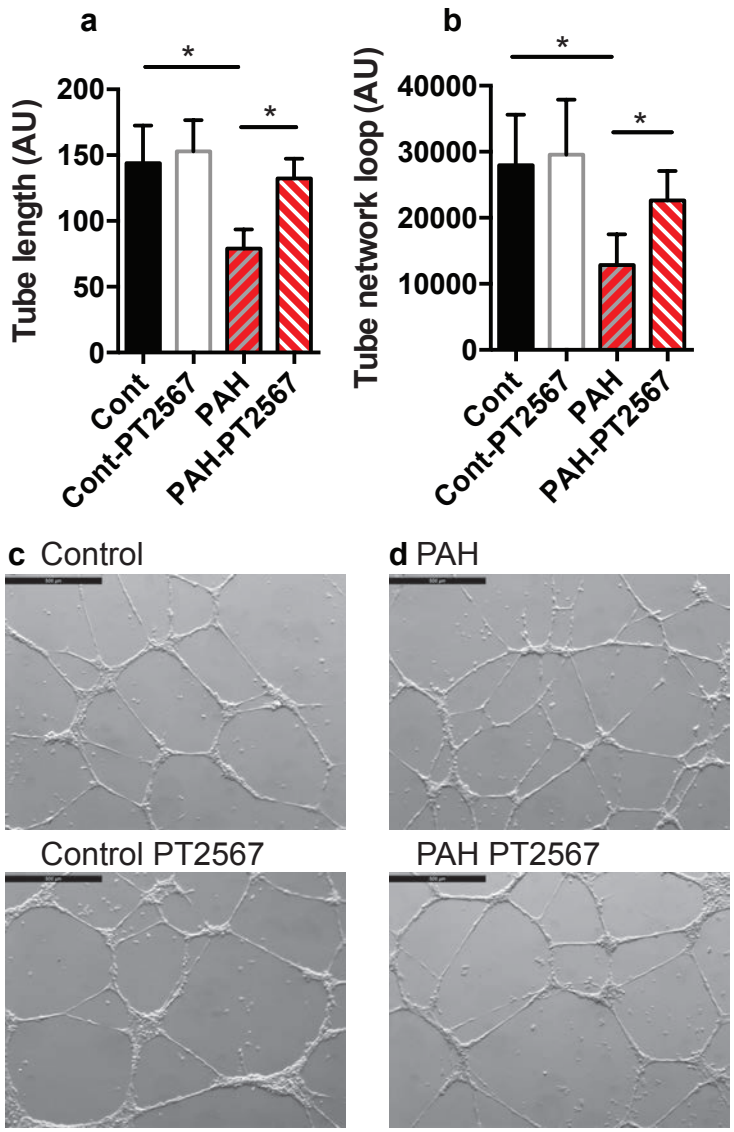

Figure S12. **PT2567 modulates aberant BOEC tube/network formation**
a Analysis of BOEC tube lengh between branch point. and b Measurment of BOEC network loop size following treatment with vehicle or PT2567 (1uM). Analysis was completed 20hr after plating BOECs.
c-d Representative photomicrographs of BOEC network formation assay from c, healthy control and d, PAH patient treated with vehicle of PT2567 (1uM)